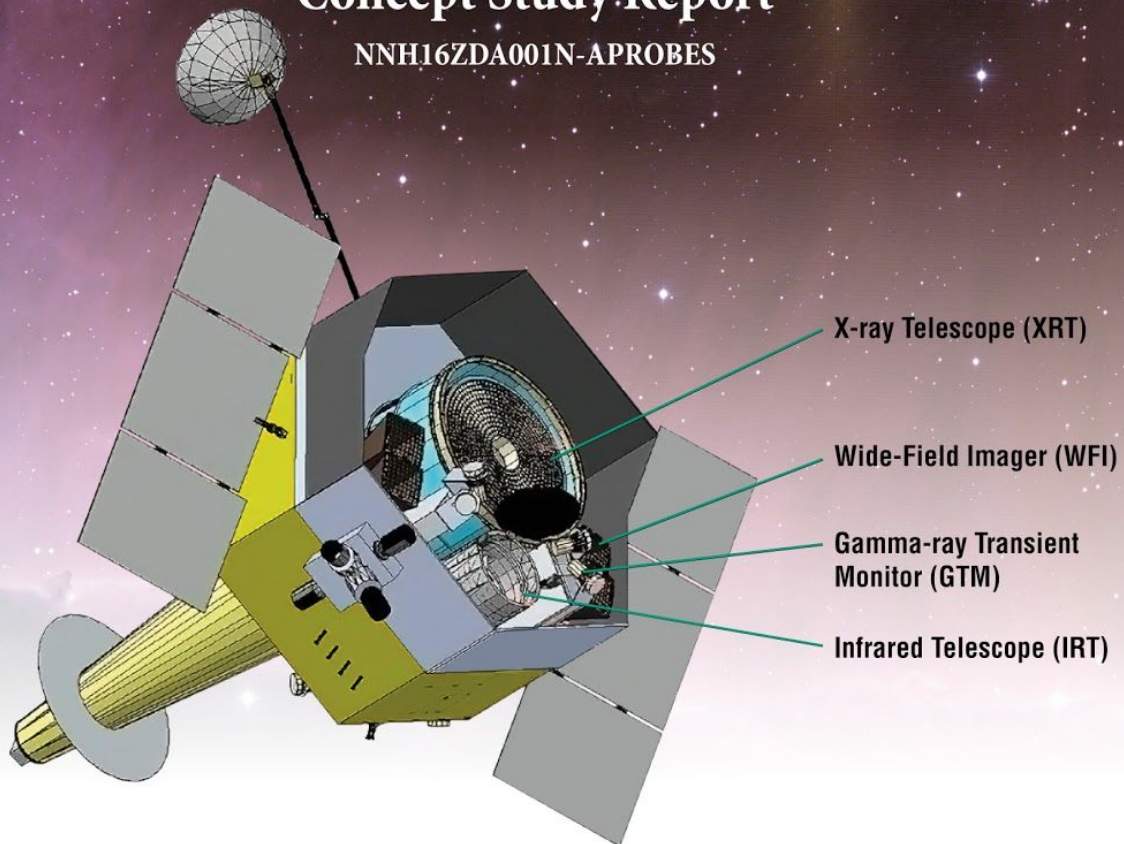


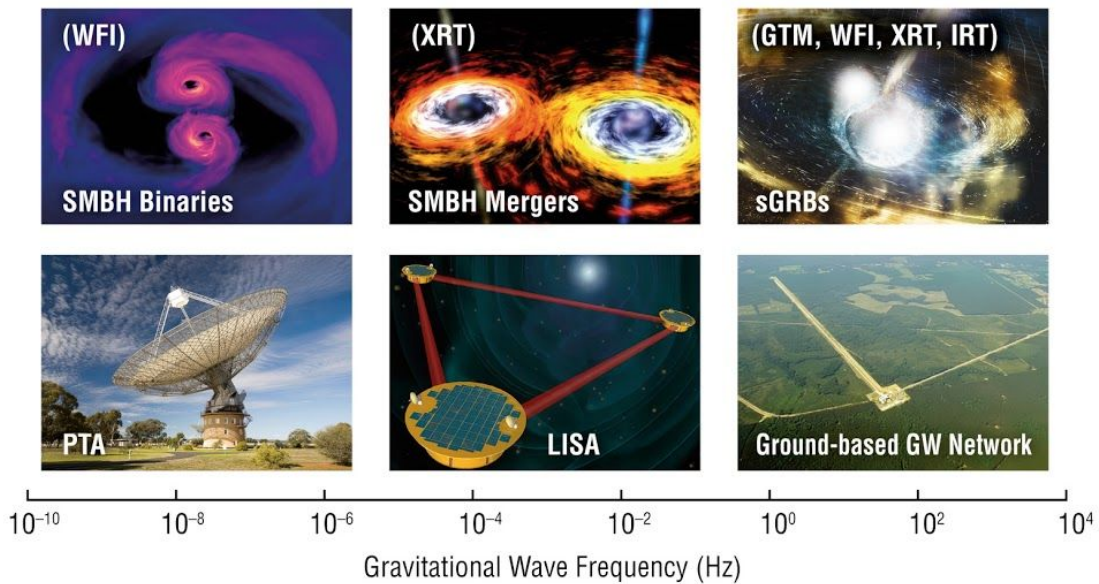
Transient Astrophysics Probe

Concept Study Report

NNH16ZDA001N-APROBES



TAP Counterparts & Gravitational Wave Telescopes



Transient Astrophysics Probe

Concept Study Report

In Response to NASA NNH16ZDA001N-APROBES

Principal Investigator: Jordan Camp

NASA-GSFC

Code 663

301-286-3528

jordan.b.camp@nasa.gov

Table of Contents

1. Executive Overview	3
2. Introduction: The Science Landscape	6
2.1 Gravitational Wave Counterparts	6
2.1.1 LIGO-Virgo-KAGRA-India Network	7
2.1.2 LISA	10
2.1.3 Pulsar Timing Array Counterparts	11
2.2 Time-Domain Astronomy	12
2.2.1 High-Redshift GRBs and the Epoch of Reionization	12
2.2.2 Tidal Disruption Events (TDEs)	14
2.2.3 Supernova Shock Breakouts	15
2.2.4 Active Galactic Nuclei (AGN)	16
2.2.5 Synergy with other Time-Domain Facilities	16
2.2.6 IR Transients	17
2.2.7 Neutrino Counterparts	17
2.2.8 Exoplanet Characterization	18
3. Observations and Measurements, Design Reference Mission, and Science Yield	18
3.1 Science Traceability Matrix	19
3.2 Source Rates	21
3.3 GW Counterparts	21
3.3.1 Ground-based GW Network	21
3.3.2 LISA	24
3.3.3 Pulsar Timing Array (PTA)	25

3.4 Time-Domain Astronomy	26
3.4.1 Gamma-ray Bursts	26
3.4.2 Tidal Disruption Events (TDEs)	27
3.4.3 Supernovae	28
3.4.4 AGN and Blazars	28
3.4.5 Novae Thermonuclear Flash	29
3.4.6 Thermonuclear Bursts	29
3.4.7 Neutrino Counterparts	29
3.4.8 Exoplanets	30
4. Instrumentation Payload	30
4.1 Wide-Field Imager (WFI)	31
4.2 Infrared Telescope (IRT)	33
4.3 X-ray Telescope (XRT)	34
4.4 Gamma-ray Transient Monitor (GTM)	35
4.5 Descoped Instrument Performance and Rates	36
4.6 TAP: a next generation transient observatory after Swift	38
5. Mission Design	38
5.1 Launch and Early Operations	39
5.2 Observatory Design	39
5.3 Spacecraft	40
5.4 Ground Stations	42
6. Concept of Operations	43
7. Technology	45
8. Risk	46
9. Project Schedule	48
10. Cost Estimate with Justification	48
List of Participants	50
References	50
Acronyms	54

1. Executive Overview

We propose here the Transient Astrophysics Probe (TAP), an observatory designed to greatly advance our astrophysical understanding of the transient Universe. TAP will feature the characterization of electromagnetic (EM) counterparts to Gravitational Waves (GW) involving mass scales from neutron stars (NS) to $10^9 M_{\odot}$ Supermassive Black Hole (SMBH) Binaries. TAP will also target a broad variety of time-domain astrophysical phenomena involving compact objects. To enable these scientific goals, we propose a multi-instrument platform, with rapid, high-sensitivity transient follow-up over a broad energy range. Wide-field X-ray (0.4 sr) and gamma-ray monitors (4π sr), a high-resolution sensitive X-ray telescope (0.8 deg^2), and a wide-field infrared telescope (1 deg^2) comprises the complementary instrument suite. This combination will discover transients deep into the Universe, and enable astrophysical characterization through broadband observations. The TAP observatory requires only one modest path of technology development (raising the XRT TRL from 5 to 6, which has been funded by NASA to be completed by end of 2020), and fits credibly within the \$1B cost cap. TAP science is directly responsive to the goals set forth by the Astro2010 Decadal Survey and the NASA Astrophysics Roadmap in the areas of gravitational waves and time domain astrophysics.

The most exciting avenue of investigation in the TAP discovery space will be the astrophysical characterization of GW signals. The recent LIGO/Virgo discovery of a binary NS merger and its subsequent Multi-Messenger follow-up has generated enormous interest in future observation of EM counterparts to GW sources. TAP will host a set of X-ray and near-IR instruments that will provide an optimal means for follow-up and localization of GW detections by the LIGO-Virgo-KAGRA-LIGOIndia network of observatories (Ground-based GW Network), as well as X-ray follow-up of detections from the planned space-based GW observatory LISA (assuming launch dates for TAP and LISA are both in the late 2020s/early 2030s). Counterparts to very massive GW sources identified by Pulsar Timing Arrays (PTAs) are also likely to be detectable. TAP will follow up all GW events expected from multiple facilities across the GW frequency spectrum, spanning the BH range from a few to billions of solar masses. The scientific output will be prodigious, including insights in cosmology, nucleosynthesis, the engines of gamma-ray bursts (GRBs), the interaction of merging accretion disks, and tests of MHD/GR models of merging compact objects.

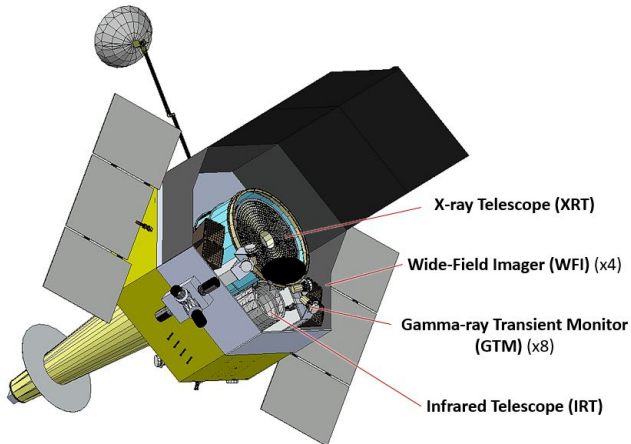


Figure 1.1: *TAP will be a powerful transient discovery machine with the capability to rapidly find, locate, and conduct broadband follow-up observations of new transients and flaring sources. The TAP mission concept is shown with the instrument suite made up of 4 WFI soft X-ray modules, the NIR IRT, the soft X-ray XRT, and 8 gamma-ray GTM detectors.*

In addition, TAP will address a multitude of transient astrophysical phenomena associated with compact objects (black holes and neutron stars; BHs and NSs) in a large range of environments, cosmic explosions (GRBs, Supernovae; SNe), and the launch and acceleration of matter in relativistic jets (Active Galactic Nuclei, AGN; Tidal Disruption Events, TDEs). Through its support of a broad user community in targeted as well as follow-up observations, TAP can be described as a “next-generation *Swift* observatory”, with each of its instruments achieving roughly an order of magnitude improvement in performance relative to the corresponding *Swift* instruments (**Table 4.3**).

The baseline TAP mission concept (**Fig. 1.1, Table 4.1**) combines the X-ray wide-field imager (WFI), the highly sensitive X-ray imaging telescope (XRT), the wide-field optical/IR telescope (IRT), and the gamma-ray transient monitor (GTM). The WFI, based on Lobster-eye grazing incidence microchannel optics, has a sensitivity of $F_{0.3-5.0 \text{ keV}} \sim 2 \times 10^{-11} \text{ erg s}^{-1} \text{ cm}^{-2}$ in 2000 s in a combined 0.4 sr field of view (FoV) that will cover at least 50% of the sky every 24 hr with 700 s exposures. The XRT ($F_{0.5-2 \text{ keV}} = 5 \times 10^{-15} \text{ erg s}^{-1} \text{ cm}^{-2}$ in 2000 s) will have a large field of view (0.8 deg^2) and $5''$ resolution. The IRT has a 70 cm diameter mirror, a wavelength range of 0.4–2.5 μm , a 1 deg^2 FoV, and is capable of multiband photometry and $\lambda/\delta\lambda=30$ slit spectroscopy. The GTM will monitor the gamma-ray (10 - 1000 keV) sky for transients, providing prompt triggering and localizations with $<20^\circ$ radius accuracy. A rapid response autonomous spacecraft ensures the fast repointing of the TAP instruments. The instrument requirements are shown in the Science Traceability Matrix (**Table 3.1**); they are obtained from the science objectives of studying the characteristics of sizable populations of gamma-ray, X-ray and optical/IR counterparts of Ground-based GW Network detections. As more counterpart data is accumulated over the next several years, the TAP instrument design may be tweaked accordingly (eg, IRT waveband, XRT and IRT FoV vs sensitivity, etc.) with minimal cost impact.

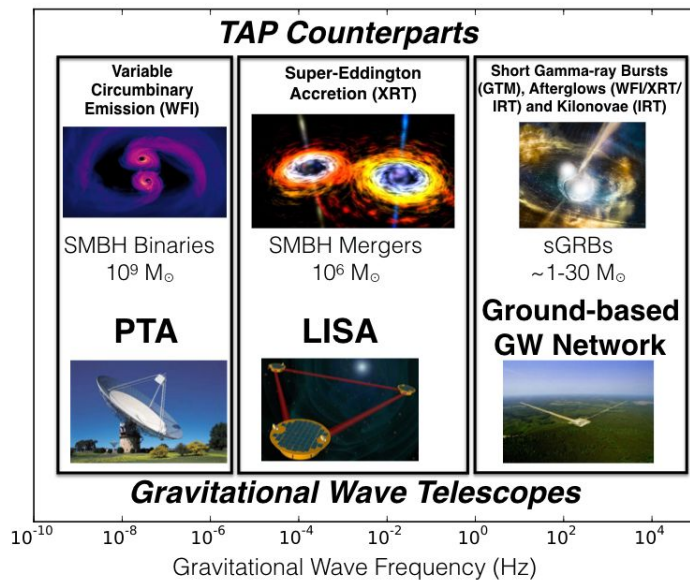


Figure 1.2: TAP will observe the electromagnetic counterparts to merging compact objects on mass scales from NSs to $10^9 M_\odot$ SMBHs, including: the mergers of NSs and stellar-mass BHs as X-ray and IR counterparts to Ground-based GW Network events (with the WFI and IRT); the merger of $\sim 10^6 M_\odot$ SMBH as X-ray counterparts to LISA detections (with XRT); and potentially as $\sim 10^9 M_\odot$ SMBH binaries counterparts to discrete PTA sources (with WFI).

TAP is ideally suited for the challenging job of detecting EM counterparts to GW signals (**Fig. 1.2**). Only the WFI technology offers a wide enough FoV along with the high sensitivity needed to efficiently cover large error regions obtained for a significant fraction of Ground-based GW Network events in the 2020s, while the 1 deg^2 FoV IRT and 0.8 deg^2 FoV XRT will be used to tile smaller sky maps with high sensitivity. While surveying the X-ray sky, the WFI may also identify several counterparts of discrete low-frequency GW sources observed by PTAs.

The wide-field, 1 deg^2 FoV IRT will be a powerful instrument for detection of predicted isotropic kilonova signatures from binary NS mergers, with a rate of ~ 1 per week. With a launch of LISA in the late 2020s to early 2030s, the sensitive, 0.8 deg^2 FoV XRT could observe counterparts (~ 1 per year) of LISA GWs from SMBH binary mergers potentially out to $z \sim 3$. TAP will find a host of EM counterpart detections to maximize the science return from the full set of GW networks.

TAP will also enable the characterization of the high redshift Universe and the epoch of reionization by detecting GRBs to redshifts $z > 10$, addressing the nature of the first stars and inhomogeneous chemical evolution during its first manifestations. It will provide a bonanza of detections of tidal disruptions and core-collapse SN (ccSN) shock breakouts, in both near (using the WFI) and deep (using the XRT) fields, at sensitivities more than a factor of 10 higher than previous instruments including the all-sky monitor MAXI and *Swift* XRT, respectively. In its survey mode, TAP will perform a deeper and wide survey of the X-ray sky, most notably AGN, whose variability determination will allow us to effectively distinguish them as candidates for LISA and PTA GW counterparts.

When TAP is not chasing newly discovered transients (onboard or following up sources from other facilities), it will conduct a broadband sky survey. There will be considerable synergy in the time-domain X-ray and IR observations afforded by TAP with other time-domain facilities including LSST (optical), and LOFAR and SKA (radio). Inspired by the model of the highly successful *Swift* mission, sensitive X-ray and IR rapid follow-up instruments will provide valuable information on each detected transient or monitored source to a broad user community. TAP's observational program is graphically summarized in **Fig. 1.3**.

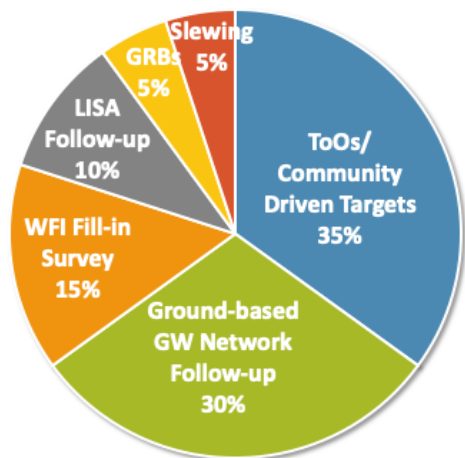


Figure 1.3: TAP has a diverse observing program made up of key science programs (GW follow-up, GRBs), filling in WFI sky survey, community observing time (ToOs), with $\sim 5\%$ of the time slewing.

TAP's cost, estimated directly from two parametric models which showed agreement at the 15% level, is ~\$1B (**Table 10.1**). TAP contains elements of previous mission studies but goes far beyond them in its science goals and instrument suite. All technologies are \geq TRL 6, with the exception of the XRT mirror, which is now TRL 5, and is funded by NASA to attain TRL 6 by the end of 2020. The TAP concept includes ~\$80M of descopes which are straightforward modifications to the instrument suite, and which yield only a modest reduction of the mission science yield (**Table 4.2**).

In summary, TAP will provide a uniquely powerful scientific capability in the revolutionary new era of Multi-Messenger Astronomy, characterizing X-ray, gamma-ray and IR counterparts of 10s/yr of Ground-based GW Network detections, as well as (plausibly) ~1/yr of LISA and several of PTA counterparts. TAP will also support a broad community of astronomers performing a wide variety of time-domain astrophysics with its multiwavelength platform of instruments on a rapid response spacecraft. TAP will operate at a time of significant capability in time-domain astronomy and interact synergistically with numerous facilities, enhancing its observations with further multiwavelength classification. Finally, TAP's design is well supported by previous detailed mission studies hosting similar instruments, and credibly fits within the \$1B Probe cost cap.

2. Introduction: The Science Landscape

2.1 Gravitational Wave Counterparts

Gravitational wave astronomy has gone from the first detection to the first catalog of events in just three years. By the late 2020s to early 2030s the detection of binary mergers by a network of ground based interferometers will be a daily event. By that time pulsar timing will likely have detected the background hum from a forest of supermassive black hole binaries, and possibly isolated a few individual systems. The LISA mission will also launch in this time frame, and is expected to detect many sources in the first weeks of operation.

The value of multiwavelength observations has been understood for many decades, and with the first multispectral observation of a neutron star merger we have a glimpse of the scientific potential of joint gravitational and electromagnetic observations.

The timescales and observing scenarios for observing electromagnetic counterparts to gravitational wave signals differ widely across the gravitational wave spectrum. The best understood targets are binary neutron star mergers observed by the kilohertz-band ground based interferometers, and it is these events that drive the TAP design. However, the versatility of the TAP design make it a powerful instrument to search for a much wider range of possible counterparts to the milli-Hertz band LISA signals and nano-Hertz band PTA signals.

For binary systems, the duration of a signal scales as an inverse power of the frequency. For LIGO and similar ground-based detectors, the signals last seconds to minutes; for LISA, months to years; and for PTAs, longer than the lifespan of an astronomer. LIGO-Virgo-KAGRA events demand rapid follow-up,

especially to capture prompt post-merger signatures, while the long duration of LISA and PTA signals offer the intriguing possibility of observing pre-merger signatures, such as the orbital modulation of emission from accretion onto black holes.

While no one instrument can cover the full range of possible GW counterparts, TAP provides comprehensive coverage of neutron star mergers, and the flexibility to search for counterparts across the GW spectrum.

2.1.1 LIGO-Virgo-KAGRA-India Network

By the late 2020s, a worldwide network of ground-based GW detectors will discover hundreds of compact binary mergers per year [Abbott *et al.* 2018]. Although the GW data alone will provide many details of the sources - such as the masses, possibly the spins, and deformability of the merging objects - it will perform a very limited probe of the environment and the baryonic and electromagnetic processes associated with the sources. Moreover, the GW data will localize the sources with limited precision: a few square degrees in the best cases and hundreds of square degrees for a considerable fraction of the discoveries. Many of the GW events will involve at least one NS and will emit EM radiation over a wide range of wavelengths. Therefore, EM observations will be necessary to place the events in their full astrophysical context and complete the picture of each future detection.

The discovery of the binary neutron star merger GW170817 demonstrated the potential of combining GW and EM observations to answer fundamental questions about astrophysics, cosmology and fundamental physics [Abbott *et al.* 2017a, Abbott *et al.* 2017b, Abbott *et al.* 2017c]. Many of these questions would still be open without EM observations. After this foundational event, multi-messenger astronomy with ground-based GW detectors and EM observatories must now be taken to a regime of routine discoveries, producing a large sample of compact binary mergers observed in both the GW and EM sectors. This sample will enhance our knowledge about the processes leading to the formation of compact objects, the behavior of matter at nuclear density, the evolution of the Universe and the origin of EM transients such as gamma-ray bursts. In order to realize such regime in a timely manner, future ground-based GW detectors need to be paired with an optimized and dedicated EM counterpart observatory like TAP.

TAP observations, in combination with ground-based follow-up EM observations, will break parameter degeneracies, independently establish source distances and energy scales, find r-process nucleosynthesis sites, and reveal host galaxies. GW170817 suggests that three kinds of EM counterpart will definitely accompany future BNS discoveries from ground-based GW detectors: short GRBs, X-ray afterglows, and kilonovae. These are the main drivers of the TAP design and are described in detail next.

Short Gamma-Ray Bursts and On-Axis X-ray Afterglows

The TAP instrumental suite presents the capability to search for on-axis X-ray afterglows with either the WFI and XRT, depending on the intensity and GW localization of the source. The WFI can be used for localization of a GW X-ray counterpart associated with a relatively large GW sky map (>100 deg²); it

then will rapidly broadcast arcmin positions to ground- and space-based instruments, including the XRT and IRT, enabling arcsec localizations, which in turn allow deep spectroscopy with large aperture telescopes. If instead the X-ray afterglow is too weak to be observed within 200 sec by the WFI, and the GW skymap is of order 25 deg^2 (as obtained with 4 or 5 GW detectors), the XRT will be used to tile the skymap with ~ 40 100 sec pointings to obtain the X-ray counterpart. This sequence will most likely yield the detection of a host galaxy. Knowledge of the redshift, host galaxy environment, and GW properties enable unique investigations of NS physics and cosmology. The relative timing between the GW merger and the GRB onset probes NS disruption (sensitive to the equation of state; EOS) [Bauswein et al. 2012; Abbott et al. 2017c], accretion disk formation, and launch timing of the relativistic jet, while the afterglow light curve reflects the angular structure and bulk Lorentz factor of the jet. The total mass of the resulting accretion torus formed during the merger depends on the NS EOS and the strength and structure of the magnetic field. The subsequent behavior of this material determines the characteristics of the X-ray afterglow, including timing, energy scale, and luminosity. The gamma-ray and X-ray signatures of NS-BH mergers are particularly sensitive to the NS EOS and the BH mass and spin, since these parameters determine whether the NS is tidally disrupted by the BH [Ruffert and Janka 1999; Janka et al. 1999; Tsang 2012].

Off-Axis X-ray Afterglows

If no counterpart is identified promptly (within ~ 1 day) by the GTM, WFI, or XRT, it may be because the narrowly collimated relativistic jet is pointed away from our line of sight. Such off-axis “orphan” afterglows can still be recovered at later times, as the lateral spreading of the jet leads to slowly rising (time scale of weeks to months) X-ray emission. The discovery of rising X-ray and radio emission associated with GW170817 [Troja et al. 2017; Hallinan et al. 2017] marked the first robust detection of such an off-axis event. In addition to serving as the first direct confirmation of our picture of GRBs as collimated outflows, these observations were critical to establishing that GW170817 was comprised a “structured” (i.e., Lorentz factor varying as a function of angle from the rotation axis) jet [e.g., Troja et al. 2018, Nynka et al. 2018, Alexander et al. 2018]. Furthermore, together with long-term radio monitoring, constraints from the late-time X-ray emission were critical in establishing the viewing angle of this event, which is a necessary input to extract precise cosmological constraints from binary neutron star mergers (e.g., Hotokezaka et al. 2018). With its sensitive XRT instrument, TAP will search for off-axis X-ray emission in the weeks and months following the merger if no other counterpart is detected.

Kilonovae

Binary mergers involving neutron stars can eject a small amount of neutron-star material via different mechanisms. The ejecta is composed primarily of neutrons and undergoes rapid neutron-captures, synthesizing very neutron-rich (r-process) nuclei. The radioactive decay of these nuclei then powers a thermal electromagnetic emission spanning wavelengths from ultraviolet to infrared, referred to as a kilonova [e.g. Metzger 2017]. The initial ejection of neutron-star mass can be driven by the tidal forces during the last few orbits prior to merger, leading to spiral-shaped ejecta located in the equatorial plane and containing a relatively low electron fraction. A second mechanism responsible for mass ejection is the violent contact between the two neutron stars at merger, which squeezes material outwards, preferentially

in the polar direction. This kind of ejecta is characterized by a larger fraction of electrons and lies mostly within a cone along the orbital axis. The remnant object at the end of the merger can produce a third type of outflow, either in the form of wind from a stable magnetar, or from some of the previously ejected material forming an accretion disk around a newly formed black hole. This outflow is expected to be more isotropic than the previous ones. Because of their different compositions and geometrical patterns, these different ejecta produce distinct electromagnetic emission and have different opacities. Thus, the overall emission has characteristics which strongly depend on the observer's viewing angle, the masses and nature of the merging objects, and the nature of the remnant object. Nevertheless, the luminosity is expected to be roughly isotropic, making the detectability of kilonovae a shallow function of viewing angle and thus much more likely compared to GRB prompt emissions.

The first definite observational proof of a kilonova associated with a neutron star merger is GW170817 (*Abbott et al, 2017b*). Earlier observations associated with GRB 130603B, but lacking the gravitational-wave confirmation, are consistent with the kilonova model [*Berger et al. 2013; Tanvir et al. 2013*]. The current observations suggest a non-negligible variance of kilonovae across different events. Although a considerable amount of evidence was gathered from these observations, in particular from the single event GW170817, several important details of the kilonova paradigm remain poorly constrained: (i) the characteristics of the ejecta (e.g. composition, angular structure, density and velocity profiles) and its relation with the properties of the objects before and after the merger; (ii) the wavelength-dependent opacity of the heavy neutron-rich nuclei, which is difficult to investigate in laboratories and to calculate on a theoretical basis; (iii) the contribution of neutron-star mergers to the abundances of heavy elements in the Universe, i.e., the role of BNS mergers for r-process nucleosynthesis.

The rate of neutron-star-merger discoveries expected for gravitational-wave detectors in about a decade offers the opportunity to greatly enhance the amount of observations in support of the above points. The kilonova observation might also be combined with the gravitational-wave data to improve our understanding of each individual merger, for instance helping to break the degeneracy between distance and viewing angle, or the ambiguity between a BNS and an NSBH merger. It is obvious, however, that future GW events will need an adequate platform to observe the associated kilonova emission. Because many events will be located hundreds of Mpc away and poorly localized in the sky, most ground-based optical telescopes and large infrared space telescopes will not be sufficient for a thorough follow-up. In contrast, TAP's IRT contains a wide FoV (1 deg²) and a sensitivity (23rd magnitude in 5 minutes) that will allow for efficient tiling of the GW skymap, and resultant localization of the source.

Other than informing the kilonova model, a discovery of the kilonova associated with a GW detection provides a precise localization of the merger, enabling the identification of the host galaxy. If a redshift measurement can be obtained from the galaxy, it can be combined with the luminosity distance inferred from the GW data to improve the measurement of the Hubble constant initiated by GW170817; 200 events would suffice to yield a precision of 1% in H_0 and resolve the tension between the present measurements. In addition, the characteristics of the host galaxy and its location with respect to the merger can be linked to the properties of the merging objects and the amount of heavy elements produced in the kilonova. A large population of events will enable the detailed exploration of these relations.

GW Detectors in 2020+

The Advanced LIGO and Virgo detectors are expected to reach design sensitivity by 2021. They will soon be joined by the Japanese KAGRA detector, and a network will be further expanded when the LIGO-India detector begins operation in the mid 2020's. Plans are in place to upgrade the instruments using the existing facilities. The NSF has approved funding for the A+ LIGO project [url#1], which aims to increase the BNS detection range by a factor of 1.7 by the mid 2020s, before TAP's launch. The increased sensitivity and the improved coverage of a world-wide network will increase the detection rates by an order of magnitude to greater than 1/week, improve the sky localization, and allow for alerts and localization information to be sent out *prior* to merger. These pre-merger alerts may allow TAP to repoint and catch the merger as it happens for several BNS events [Cannon, 2012, Chan, 2018].

2.1.2 LISA

Unlike stellar-mass BHs, which are expected to reside in gas-poor environments, there is substantial theoretical motivation for there to be significant gas near and thus electromagnetic counterparts to the massive BH binaries formed at the centers of merging galaxies. With a space-based interferometer like LISA, we expect to see gravitational waves from relatively lower-mass systems ($10^{6-7} M_{\odot}$ as opposed to the quasar-scale masses of 10^8-10^9). With TAP alone, we would have essentially no chance of finding these faint objects. Yet with coordinated observations from LISA, TAP will enjoy an early-warning system that will give error boxes on the order of a few degrees as much as several days before the binary BH merger. This will allow focused observations with the XRT and IRT. For binary systems with non-trivial amounts of gas in the vicinity, prompt signatures are likely. They have peak luminosities comparable to those of TDEs (i.e. many times Eddington), with signals expected to vary over a few dynamical times near merger (~ 1 hr for a typical $10^7 M_{\odot}$ LISA source).

With an electromagnetic counterpart detected by XRT, the host galaxy for the LISA signal can be identified. Measuring the host galaxy redshift opens up a wide variety of possible science applications, testing fundamental physics and cosmology. Depending on the specific formation mechanisms responsible for $z < 3$ SMBH, we expect to detect and localize several of these sources with LISA and TAP coordinated observations spanning a 5 yr mission [Dal Canton *et al.* 2019]. These observations will provide strong constraints on the leading models of BH formation and evolution in cosmic time.

In addition to the simultaneous observations of EM counterparts to LISA sources, TAP will also be able to identify and monitor candidate SMBH binaries that are still many thousands of years before merger. Because of their long lifetimes, these precursor systems are expected to be far more numerous than the actual merging LISA sources, and thus should be located at much closer distances. While theoretical models of such sources are still in their infancy, they are expected to resemble normal AGN in many regards, but also have strong X-ray variability on timescales of weeks to months, ideal for observations with TAP [url#2].

Galactic white-dwarf binaries represent another potential source of multi-messenger observations with LISA and TAP. Once identified and roughly localized by LISA, a fraction of these systems might be

discovered by TAP via eclipses and modulations in their optical light curves [Littenberg *et al.* 2012, Korol *et al.* 2017]. Such observations would complement the information provided by LISA, for example constraining the size of the white dwarves and measuring their tidal heating [Cooray *et al.* 2004]. LISA will also observe compact remnant (black hole or neutron star)/white dwarf binaries that have been suggested as sources of either weak gamma-ray bursts [Fryer *et al.* 1999] or Ca-rich supernovae [Metzger 2012]. TAP electromagnetic observations will be able to distinguish these fates.

2.1.3 Pulsar Timing Array Counterparts

SMBH binaries are the most energetic GW sources in the Universe. The systems most likely to be detected with PTAs will have particularly high masses ($\geq 10^8 M_\odot$), long periods ($T_{\text{orb}} \geq 1$ yr), and reside in the local Universe ($z \lesssim 1$). As a population, these sources are expected to combine to produce a stochastic signal at nanoHertz frequencies, with characteristic strain amplitude around $h \sim 10^{-15}$. At the current rate of PTA improvements (a combination of hardware improvements, more/better pulsar targets, and longer time integration), the stochastic background could very well be detected by 2024 [Taylor *et al.* 2016].

The first individually resolvable sources should be detectable shortly thereafter, and will mostly likely represent the high-mass, short-period, most nearby outliers from the stochastic population. These features are also the most favorable for bright EM counterparts, which should be easily detectable with existing ground- and space-based telescopes. The WFI will provide independent candidates that can be used to lower the threshold for PTA detections of resolvable binary sources. A $10^9 M_\odot$ BH accreting near the Eddington limit at a distance of 1 Gpc will produce an X-ray flux (10% bolometric correction assumed) of roughly 10^{-12} erg sec $^{-1}$ cm $^{-2}$ [Schnittman 2014]. This is detectable with the WFI for week-long integrations, and well within the sensitivity of the XRT. Large-scale MHD simulations of circumbinary accretion disks are still in their infancy, but most results suggest that (quasi-)periodic accretion is to be expected on orbital timescales with X-ray modulation amplitude of order unity [Bowen *et al.* 2018].

As with identifying LISA precursor sources, the primary challenge of observing EM signatures from SMBH binaries lies in correctly identifying and characterizing binary sources with long orbital periods, as opposed to "normal" AGN hosting single BHs. Here too TAP will provide valuable new understanding into the wide range of behaviors seen in AGN by vastly expanding our sample of X-ray light curves from accreting SMBH.

2.2 Time-Domain Astronomy

With the 2020s bringing about an era of wide-field survey telescopes across the EM spectrum (LSST in optical, WFIRST in NIR, SKA in radio), a high-energy counterpart discovery machine like TAP is needed to both *detect* and *follow up* transient and variable sources in cooperation with these other facilities. In this section we describe a subset of the time-domain science possible with TAP (with particular emphasis on those topics that drive instrument and/or mission requirements). However, we stress that we cannot capture the full breadth of transient science possible for such a versatile mission, in particular when working in concert with facilities like LSST and the SKA (§2.2.6).

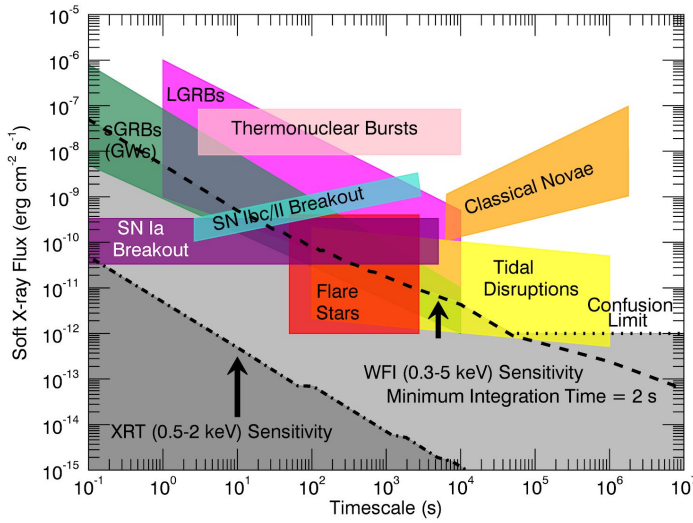


Figure 2.1: *TAP probes the sky for many Galactic and extragalactic transients (rates in [Table 3.2](#)) with a wide range of variability timescales from seconds to months, and complements multi-wavelength surveys. The WFI, XRT and IRT will be able to detect many of these sources during survey operations, and the XRT and IRT will be able to follow up WFI sources as they fade over the hours, days, and months afterwards.*

2.2.1 High-Redshift GRBs and the Epoch of Reionization

The 2010 Decadal Survey identified the “[search] for the first stars, galaxies, and black holes” as the highest priority scientific objective for the current decade. Of particular importance is to understand the timescale and source population responsible for cosmic reionization. GRBs can serve as unique probes of this critical era in the evolution of the Universe. Because their afterglows are remarkably bright, GRBs have been detected out to redshift 8–9 [[Salvaterra et al. 2009](#), [Tanvir et al. 2009](#), [Cucchiara et al. 2011](#)], and thanks to their simple power-law energy spectra, GRBs serve as a reliable probe of high-redshift Lyman break galaxies, as they reveal galaxies independent of host luminosity.

By measuring the profile of the Ly α absorption feature (as well as the transmission down to the Ly limit) in the spectra of high-redshift GRBs, it is possible to infer the neutral H fraction of the intergalactic medium, X_{IGM} , along the line of sight. Even with only a few events with sufficiently high SNR (and spectral resolution) to date, GRBs already provide comparable constraints on X_{IGM} to that obtained from the ensemble population of quasars at $z \approx 6$ [[Chornock et al. 2014](#)] (**Fig 2.2**).

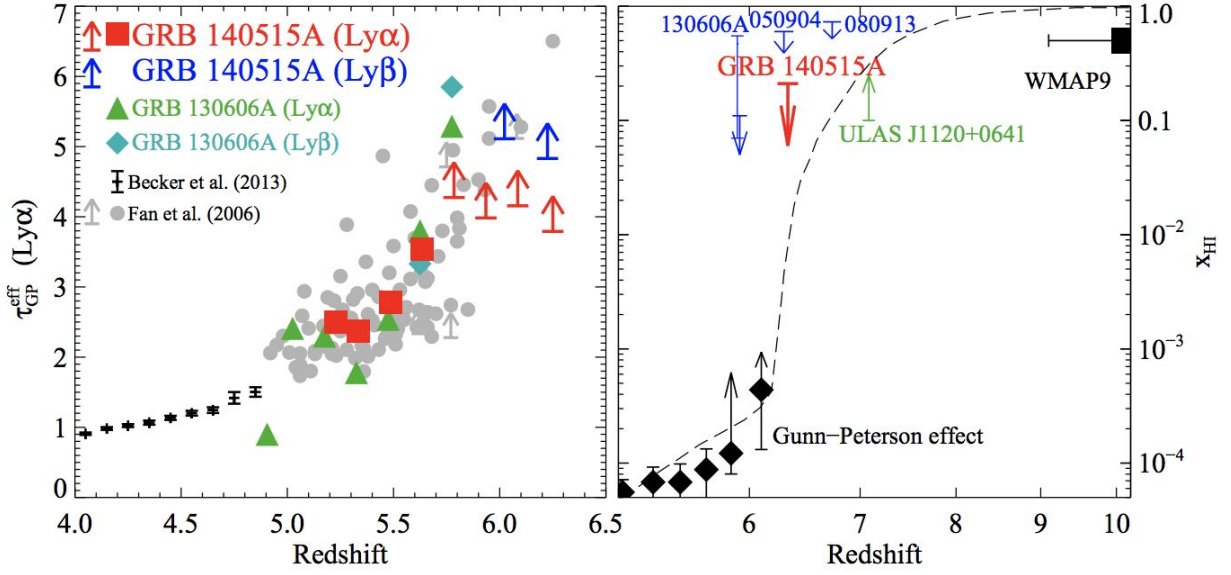


Figure 2.2: Redshift evolution of the IGM. Left: Ly α effective optical depth, as measured from quasars (grey and black points) and two $z \approx 6$ GRBs. Right: Neutral fraction of the IGM, as measured by quasars (black diamonds and green limit), WMAP (black square), and GRBs (blue and red limits). Even with only two GRB spectra with sufficient SNR and resolution, comparable constraints to the ensemble quasar population are obtained. TAP will populate the redshift space between $z \approx 6-10$ with dozens of sight lines.

Further progress requires a sample of events over the redshift range from $z \approx 6-10$, where we know (from the CMB and quasars) that the bulk of reionization occurred (Fig 2.2). While such distant events have been found by current GRB satellites (e.g., *Swift*), no $z > 7$ GRB has been identified promptly enough to obtain a high SNR, moderate resolution spectrum to obtain a cosmologically interesting measurement of X_{IGM} . Furthermore, because reionization is expected to be “patchy”, a sizeable sample of events is necessary to address cosmic variance (or, alternatively, to place limits on the bubble size and thus the source of ionizing photons [McQuinn et al. 2008]).

In addition to measurements of the IGM, the large afterglow luminosity and simple power-law spectra also enable detailed measurements of the local environments in which these first massive stars formed (i.e., the ISM). With TAP’s on-board IR imager and spectrograph, *bonafide* high-redshift GRBs will be promptly identified for detailed characterization with sensitive space- (JWST, ATHENA) and ground-based (giant segmented mirror telescopes). Absorption spectra of such events are unique probes of the composition (e.g., metallicity) of distant galaxies, and highly complementary to emission-line studies that will be conducted by facilities like JWST in the coming decade.

2.2.2 Tidal Disruption Events (TDEs)

When a star is scattered into the tidal radius of a SMBH, tidal forces will tear the star apart. If the SMBH is too massive ($M_{\text{BH}} > 10^8 M_{\text{Sun}}$), this disruption will occur inside the event horizon, hidden from outside

observers. However, for less massive black holes, the bound debris will accrete and emit a flash of radiation known as a tidal disruption event [TDE; *Rees 1988*].

TDEs are of broad astrophysical interest for two primary reasons. First and foremost, TDEs serve as signposts, pointing the way towards SMBHs in distant galaxies that may not otherwise be detectable. In the nearby Universe ($d < 100$ Mpc), kinematic studies of stars and/or gas in the central few parsecs of quiescent galaxies have revealed that BH mass is correlated with the mass of the host bulge; this is known as the $M_{\text{BH}}-\sigma$ relation, since bulge masses are proxied by the velocity dispersion of bulge stars [*Ferrarese et al. 2000; Gebhardt et al. 2000*]. Yet the underlying mechanisms connecting galaxy growth (fueled at least in part by mergers) with black hole growth (fueled by accretion) remain a mystery. TDEs may offer an independent probe that can extend SMBH measurements beyond the resolution limits of current facilities. For example, in simple analytic models M_{BH} should scale as the square of the rise time of the light curve.

Second, TDEs serve as a powerful probe of the accretion process itself. Unlike AGN and X-ray binaries, the accretion resulting from a TDE is deterministic, and the rate that mass returns to the SMBH is straightforward to derive ($\propto t^{-5/3}$). For many systems the accretion rate is predicted to transition from highly super-Eddington to sub-Eddington on a time scale of months to years. Thus, in a single SMBH, we can search for analogs to the “state transitions” observed from stellar-mass black holes, but on a time scale orders of magnitude shorter than AGN are thought to turn on and off.

To date, there are ~ 70 claimed TDE detections with ground- and space-based observatories (e.g., *Gezari et al. 2008, The Open TDE Catalog*¹). However, only a handful have well sampled light curves that measure the rise-time to peak [e.g., *van Velzen et al. 2018*], or multiwavelength detections that probe the broadband spectral energy distribution of the flares [e.g., *Holoien et al. 2016*]. Furthermore, the bulk of these discoveries have been made by wide-field optical surveys, and the origin of this optical emission (which is much more luminous than expected for thermal emission from an accreting tidal debris disk) remains hotly debated.

A large sample of X-ray-selected TDEs *with well-measured rise-times*, as provided by TAP, is critical for a number of reasons. First, TDEs from the low end of the SMBH mass function (10^4 - $10^5 M_{\odot}$, i.e., the intermediate mass black hole regime) are visible only in the X-rays, because the peak of the spectrum is in the X-ray band. As a result, an X-ray sample will uniquely measure the BH occupation fraction in dwarf galaxies, a critical link in our understanding of the connection between the evolution of galaxies and SMBHs.

Second, *Swift* has shown that a fraction of these events also launch relativistic jets [*Bloom et al. 2011; Burrows et al. 2011; Zauderer et al. 2011*], which are thousands of times more luminous than non-jetted TDEs and emit the bulk of their energy at soft X-ray wavelengths. Understanding the conditions that lead to the formation of relativistic jets from accreting black holes will therefore require wide-field X-ray coverage like that provided by the WFI and XRT on TAP.

¹ <https://tde.space/>

Finally, TDEs are also closely linked to a specific class of LISA sources called extreme mass ratio inspirals (EMRIs). EMRIs are formed when a SMBH in the center of a galaxy captures a stellar-mass BH, which proceed to merge via the emission of gravitational waves. In both the TDE and EMRI systems, the smaller object comes into close contact with the central BH via dynamical processes in the galactic nuclei, so the rates should be closely related. Given the significant uncertainty in the origin of the UV/optical emission in these systems, accurate rate estimates require large X-ray samples of TDEs.

2.2.3 Supernova Shock Breakouts

Supernovae (SNe) are critical to our understanding of a variety of topics in modern astrophysics. Type Ia SNe, the thermonuclear explosion of a white dwarf, are used as standardizable candles for precision cosmology, having provided the first evidence for the accelerating expansion of the Universe [*Riess et al. 1998, Perlmutter et al. 1999*]. With their massive star progenitors, core-collapse SNe are responsible for the production of heavy elements and high-energy cosmic rays, and also regulate galaxy growth via feedback. However, more than half of these cosmic explosions lack robust progenitor identifications, limiting our understanding of topics ranging from stellar evolution to dark energy.

Core-collapse SNe are classified based on their optical spectra into three categories: H-rich (Type II), H-poor but He-rich (Type Ib), and H- and He-poor (Type Ic; *Filippenko 1997*). Type II SNe have firmly established progenitors from direct detection in pre-explosion images: supergiant stars (red supergiants for Type IIP SNe, blue supergiants for 1987A-like SNe; *Smartt 2015*). However, to date, direct progenitor identification has failed in all but two H-poor core-collapse SN (Type Ib/c), leaving unanswered such basic questions as: How does binarity impact the final stages of stellar evolution in massive stars? What are the progenitor stars of long-duration GRBs? What powers the so-called “superluminous” supernovae?

The discovery of shock breakout emission, the very first EM signal from a SN explosion, offers the best hope of measuring fundamental properties of the progenitor system [*Waxman & Katz, 2017*]. The luminosity and duration of the shock breakout signal directly encode the progenitor structure at the time of collapse, especially the transition region between the edge of the star and the stellar wind. For massive compact stars (with and without a thick wind), the shock breakout signal can peak in the X-rays, as detected in SN2008D [*Soderberg et al. 2008*]. Both the WFI and XRT on TAP will be sensitive to these signals, directly measuring progenitor radii for dozens of core-collapse supernovae each year.

TAP may also directly discover the predicted [*Kasen 2010; Piro, Chang, and Weinberg 2010*] hour-long X-ray emission from Type Ia (thermonuclear) supernovae when the ejecta collide with the companion star. The resulting luminosity (and timescale) is proportional to the companion radius - as a result, the detection of such outbursts would strongly indicate a non-degenerate companion star (i.e., the “single degenerate” channel for type Ia SNe). Resolving the single vs. double degenerate progenitor question for thermonuclear supernovae would have a major impact on their utility as cosmological standard sirens.

2.2.4 Active Galactic Nuclei (AGN)

Type I AGN are understood to be unobscured accreting SMBHs with a direct line of sight to their central engine, characterized by a strong X-ray component (typically >10% of the bolometric luminosity) and variable over a wide range of timescales [Beckmann & Shrader 2012], from hours to years. Historically, AGN light curves have come from intensive, targeted campaigns focused on a few bright sources [Markowitz & Edelson 2004; McHardy et al. 2006; Körding et al. 2007]. The low-frequency end of their power density spectra appear to be red noise power laws, flattening below a characteristic frequency that scales with BH mass. Joint X-ray and optical/IR monitoring also probes emission reprocessing mechanisms and the geometry of the central engine [Breedt et al. 2010]. The WFI will be able to monitor ~500 of these bright AGN on a weekly basis, and the brightest ~80 of these on a daily basis.

Peretz & Behar (2018) recently showed that different types of AGN, including radio loud (RL) AGN, Seyfert Is and IIs, as well as LINERs can be identified based on their hardness ratio behavior with time and with brightness. For example, Seyferts tend to be harder when brighter, unless their variability is driven by obscuration when they are harder when fainter (absorbed). Conversely, jetted (RL) sources tend to have a constant hardness ratio despite dramatic flux changes. However, all previous samples were based on archival light curve of “preferred” or “favorite” sources. The wide field of the WFI and its continuous monitoring will provide for the first time unprecedented numbers of such light curves and hardness ratio slopes for what will be a statistically complete and unbiased sample.

One of the great science results that would naturally emerge from such a large, unbiased time-domain survey of AGN is a much-improved understanding of their range of variability behaviors and classes. This will allow us to quantify the significance of any periodic signals seen in these light curves, in turn allowing us to identify binary SMBH candidates for more detailed multi-wavelength study.

Since TAP will be tiling the most of the sky both during searches for transient events and between observation, in general there will ~100 pointings per day with exposure of ~700 s. This will constitute a wide-area soft X-ray covering thousands of square degrees every day with a F(0.5-2.0 keV) flux limit of 1×10^{-14} erg cm⁻² sec⁻¹. The WFI will be able to detect thousands of AGN on daily timescales, >10⁴ if accumulating deep fields, and XRT would be able to detect many more at lower flux levels. These can be monitored over timescales of years during the TAP prime mission and relative to fluxes detected by eROSITA (to be launched in the 2019-2020 time frame) in the X-ray and ground surveys like LSST in the optical/NIR, exploring accretion duty cycles on 5-10 year time scales. eROSITA will perform an all-sky survey over four years with a limiting flux of 1×10^{-14} erg cm⁻² sec⁻¹ so comparable to the TAP daily XRT flux limit (over ~ 100 sq. deg.). The TAP instruments will also detect hundreds of blazars, which have a lower spatial density, but are more luminous.

2.2.5 Synergy with other Time-Domain Facilities

TAP has myriad synergies with the two wide-field time-domain surveys that will revolutionize astronomy in the 2020s: LSST and the SKA. LSST will generate transient and variable alerts at an astounding rate: ~ 10⁵ new transients each night (and orders of magnitude more known variables). TAP can provide

multi-wavelength (archival) context to help classify new LSST transients: for example, the presence/absence of a contemporaneous GRB will help differentiate on-axis from orphan afterglows, while past X-ray variability can help distinguish AGN from TDEs. For the most interesting LSST transient discoveries, TAP can provide prompt (\sim minutes), multiwavelength *follow-up* to assist with characterization (e.g., broadband spectral energy distributions for TDEs). And TAP will conduct daily *co-observing* of an LSST “deep drilling” field (e.g., COSMOS, CDF-S, depending on ground-based visibility) to perform broadband reverberation mapping measurements of bright AGN.

Similarly, the radio bandpass is naturally synergistic with the high energies probed with TAP. The latter corresponds to the natural energies of the particles in the sources, while the former is produced by synchrotron emission of those particles moving in magnetic fields or coherent radiation from very compact structures. In recent years radio astronomy has undergone a renaissance: nearly all major radio facilities have recently been upgraded and several new facilities have been and are being built, culminating with the SKA. The sensitivity, broad frequency range, large field of view and agility of the SKA will be perfectly suited for coordinated observations with TAP. For deep follow-up observations of interesting sources found by TAP, the Karl G. Jansky Very Large Array will remain a great workhorse facility into the 2030s.

2.2.6 IR Transients

Even with a modest ~ 70 cm aperture, the TAP IRT will be one of the most sensitive facilities operating in terms of limiting magnitude for an isolated point source, comparable to e.g., MOSFIRE on the 10m Keck I telescope. Together with its rapidly slewing spacecraft bus, the IRT will fill a unique void in the time-domain landscape: rapid-response, sensitive NIR imaging of transient and variable phenomena.

A wide variety of additional science will be enabled by a sensitive, wide-field IR telescope on a fast-slewing spacecraft. A few of these possibilities are: the discovery of pair-instability supernovae from extremely massive stars in the early Universe [Tanaka *et al.* 2012], dust echoes from the flares generated by the tidal disruption of stars by SMBHs in inactive galaxies [van Velzen *et al.* 2016], unveiling the nature of intermediate luminosity red transients [Thompson *et al.* 2009], IR follow-up of transients discovered by LSST and the SKA (e.g. dust-obscured SNe, orphan GRB afterglows).

2.2.7 Neutrino Counterparts

The discovery of a diffuse, cosmic flux of energetic ($> \text{TeV}$) neutrinos by IceCube [Aartsen *et al.* 2013] has led to a revival of models studying the sources of these VHE neutrinos [for reviews, see Halzen 2017 and Meszaros 2017]. Production of VHE neutrinos requires the same astrophysical conditions believed to produce high energy cosmic rays, and the production sites of both of these high energy particles are thus expected to be similar, including a large number of transient/variable astrophysical source classes: active galactic nuclei, gamma-ray bursts, failed gamma-ray bursts (a.k.a. choked jets), supernovae, and tidal disruption events. Although it is believed that conditions that drive cosmic ray acceleration (e.g. Fermi acceleration in shocks) is required, the exact conditions, and hence the most likely origin of cosmic ray and high energy neutrino production is not yet known. Broadband electromagnetic follow-up of any neutrino detection is critical to understand these properties and TAP

will provide important IR observations of these sources. The discovery of a flaring blazar (TXS 0505+056) associated with the IceCube event IC-170922 [Artsen *et al.* 2018] has pushed a new MMA window wide open, and it is urgent to be ready for the next neutrino-gamma coincidences to reveal the astrophysical sites through multi-wavelengths follow-up.

2.2.8 Exoplanet Characterization

TAP's powerful multiwavelength instrumentation will enable compelling investigations in a broad range of astrophysics, beyond the transient astronomy which is the mission's core science, and will thus appeal to a very wide user community. We describe an example of one such investigation in exoplanet characterization.

Looking forward to the next 10 years, the JWST will be the premier facility for detailed transiting exoplanet characterization, surpassing the capabilities of *Hubble* and *Spitzer*. However, the JWST is a multi-purpose facility with very broad science goals. Like *Hubble*, it is anticipated that $\leq 25\%$ of its observing time will be spent on exoplanet science, likely to characterize the most ideal targets in great detail. This aspect of the JWST, coupled with the eventual retirement of *Hubble* and *Spitzer*, provides an opportunity for additional and complementary space-based capabilities to perform detailed exoplanet characterization. The IRT on TAP has the potential to fill this gap and provide a key platform for transiting exoplanet science into the next decade. The current design of the TAP IRT, driven by the requirements for time domain photometry and spectroscopy of faint high energy transients, is well suited to measuring the transits of *known* exoplanets orbiting *bright* host stars, like those now being discovered by the Transiting Exoplanet Survey Satellite (TESS). The photometric and spectroscopic capabilities of IRT will allow for multiwavelength transit measurements to characterize these exoplanets. This includes transit spectroscopy to measure atmospheres, transit timing variations for mass measurements, phase curve and secondary eclipse measurements to detect planet thermal emission.

3. Observations and Measurements, Design Reference Mission, and Science Yield

TAP is designed to 1) discover new transients and allow their follow-up and characterization; and 2) provide a rapid follow-up facility for transients from external triggers. Both functions are enabled with TAP's four instruments covering near UV through optical and near IR, soft X-ray, and gamma-ray bands. The design requirements for the instruments and mission are largely motivated by maximizing the chance of detecting and characterizing counterparts to NS-NS mergers, with some additional requirements from the X-ray all-sky survey. The incredible first glimpse at the counterparts to GW170817 helps guide expectations for both on- and off-axis events within the detection volume of the GW network in the late 2020s.

3.1 Science Traceability Matrix

This Science Traceability Matrix (STM) describes how the primary TAP science goals drives instrument and mission requirements. It is, essentially, a summary of how the core mission science drives the mission design. The flowdown through this table, proceeding from left to right, includes:

- Science goals: the understanding of the astrophysical context associated with sizable populations of EM counterparts to NS-NS GWs detected by TAP; and also the astrophysics of TAP sources observed through its sky survey
- The science objectives associated with the above goals, including source detection rates
- The flowdown of measurement requirements necessary to achieve the source detection rates
- The flowdown of instrumental requirements to support the measurement requirements
- The flowdown of mission requirements to support the instrumental requirements

The requirements flowdown yield instrument capabilities that are eminently doable: the Wide-Field Imager has been designed in a Phase A study for the ISS-TAO proposal; the XRT has been designed in a MIDEX proposal for the mission Star-X, while requiring a modest amount of technology development that has been funded by NASA for completion by 2020; the IRT is a straightforward concept that can easily be realized by any one of a number of industrial partners; and the GTM is based on the Fermi-GBM design that has flown successfully for the past 10 years. The instrument parameters can be easily modified to reflect a deeper understanding of the EM counterparts to Ground-based GW Network events as more are discovered in the next several years before the TAP mission starts.

The mission design is also straightforward, using a conventional spacecraft designed for rapid slewing, and easily able to host the mass, power and communications consistent with the TAP flowdown of mission requirements. The mission will be in an L2 orbit and will have 4 ground stations with dedicated time that will ensure 24/7 continuous contact for immediate upload of Target of Opportunity locations and the downloading of transient alerts. The mission enabled by the combination of instruments and parameters called out in the STM will be an extremely powerful and flexible facility for the identification and characterization of astrophysical transients.

Table 3.1: *Science Traceability Matrix. It contains the current best estimate of the instrument and spacecraft design values for the various design parameters. These values were used throughout the CSR to derive the science performance and results.*

Science Goals	Science Objectives	Measurement Requirements	Instrument Requirements	Mission Requirements
Understand the populations of EM counterparts to NS-NS GW sources and use them to probe fundamental physics, neutron star physics, cosmology, heavy-element nucleosynthesis, jet physics, black hole formation, GRB production. (The rates for the other types are covered by these requirements.)	Detect prompt emission from 20/yr sGRBs in coincidence with GWs from NS-NS mergers	Gamma-ray: Energy: 10-1000 keV F_{lim} (1s): < 1.0 ph/cm ² /s FoV: 4π sr Localization: < 20°	GTM: (x8 detectors) Energy: 10-1000 keV A_{sens}: 300 cm ² / detector (100 keV) FoV: 2π sr / detector Energy Resolution: < 20% Temporal Binning: 0.25, 0.5, 1, 4 s Temporal Resolution: < 1 msec Localization: < 20° radius (90%) Data Rate: < 0.2 GB/day Mass: < 69 kg, Power: < 63 W	Mission Duration: 5 year (10 year consumables) Launch Vehicle: EELV Orbit: L2 Halo Propulsion: 200 m/s Communications: Command Availability: > 98% Low Rate Tlm Availability: > 98% Low Rate Tlm Rate: > 1 kbps Detection Latencies: < 10 sec Science Data Volume: < 8 GB/day Science Data Latency: < 24 hr Storage: 16 GB + 200 Gbit Time Accuracy: < 1 msec Pointing Control: Stability: <1 arcsec in 6 s Accuracy: <1 arcmin Knowledge: < 10 arcsec Slewing: <70 s slew 50° and settle Timing Accuracy: 100 us Resources: Available Payload Power: > 1057 W Available Payload Mass: > 833 kg
	Detect >20/yr on-axis sGRB afterglows associated with GWs from NS-NS mergers	X-ray (wide/shallow): Energy: 0.3-5 keV F_{lim} (700 s): < 4x10 ⁻¹¹ ergs/cm ² /s FoV: >36.2° x 36.2° = 0.4 sr FoR: Full sky w/ 45° Sun exclusion Spatial Resolution: < 9 arcmin (FWHM) Centroid Accuracy: < 1.5 arcmin (1σ)	WFI: (in 4 modules) Energy: 0.3 - 5.0 keV A_{eff}: > 2.4 cm ² (central core) FoV: >18.6°x18.6° / detector (w/ 1° overlap) FWHM: < 9 arcmin Data Rate: < 5 GB/day Mass: < 207 kg, Power: < 359 W	
	Detect >7/yr off-axis sGRB afterglows associated with GWs from NS-NS mergers	X-ray (narrow/deep): Energy: 0.2 - 10 keV F_{lim} (2 ks): <4.8x10 ⁻¹⁵ erg/cm ² /sec FoV: > 1° dia. FoR: Full sky w/ 45° Sun exclusion Spatial Resolution: < 5 arcsec (HPD) Centroid Accuracy: < 2 arcsec (1σ)	XRT: Energy: 0.2 - 10 keV A_{eff}: 1800 cm ² (on-axis, 1 keV) FoV: >1° dia. Spatial Resolution: < 5 arcsec (HPD) Centroid Accuracy: < 2 arcsec (1σ) Data Rate: < 0.3 GB/day Mass: < 382 kg, Power: < 481 W	
	Detect >70/yr kilonovae associated with GWs from NS-NS mergers	Infrared (near-IR and visible) Band: 0.4 - 2.5 μm F_{lim} (300 s): > 23 mag FoV: >1°x1° FoR: Full sky w/ 45° Sun exclusion Spatial Resolution: < 1 arcsec Centroid Accuracy: < 1 arcsec	IRT: Band: 0.4 - 2.5 μm Diameter: 0.7m, F/#: 3.3 FoV: >1°x1° FWHM: < 0.22 arcsec @ 0.6 μm Internal Jitter Mitigation: 20Hz FSM Data Rate: < 1.1 GB/day Mass: < 176 kg, Power: < 155 W	
Survey the Transient X-ray Sky	AGN monitoring TDE detection	X-ray (wide/shallow): F_{lim} (700 s): < 4x10 ⁻¹¹ ergs/cm ² /s Coverage: >50% sky / 24 hr >90% of the avail.sky / week	WFI (700 s integration)	

3.2 Source Rates

Assuming the projected performance in **Table 3.1**, we calculate our best estimates of the rate per year (unless specified otherwise) for the discovery and/or detection of each source class as shown in **Table 3.2**, relying on the observational timescale/pointing listed in **Table 3.5**.

Table 3.2: *Estimated rates of sources discovered by the TAP instruments.*

Transient Type	WFI Rate (yr ⁻¹)	XRT Rate (yr ⁻¹)	IRT Rate (yr ⁻¹)	GTM (yr ⁻¹)
Objective 1 – X-ray and IR Counterparts to Gravitational Wave Sources				
GW NS-NS (on-axis)	20	24	20	20
GW NS-NS (off-axis)	--	7	70	2
GW SMBH-SMBH (10 ⁶ M _⊙)	--	~1	--	--
GW SMBH-SMBH (10 ⁹ M _⊙)	Several over 5 year mission	--	--	--
Objective 2 - Highest Sensitivity Time-Domain Survey of the Transient Soft X-ray Sky				
ccSN shock breakout	1	19	--	--
Jetted TDEs	106	1	--	--
Non-jetted TDEs	1	48	--	--
AGN (daily / weekly)	120 / 660	1600 / 8700	3000 / 3x10 ⁴	--
Blazars (daily / weekly)	100 / 360	20 / 65	300 / 3000	--
Novae Thermonuclear Flash	1.1	--	--	--
Thermonuclear Bursts	400	--	--	--
Long GRBs	320	320	320	150
High-z GRBs (z>5)	25	--	22	--
Short GRBs	30	30	15	30
Off-axis Long GRB Afterglows	--	40	--	--
High-z Superluminous SNe	--	--	10	--
Dust-enshrouded transients	--	--	100	--

3.3 GW Counterparts

3.3.1 Ground-based GW Network

TAP will be sensitive to nearly all of the different electromagnetic signals associated with the merger of two neutron stars: a short gamma-ray burst [*Eichler et al. 1989; Paczynski 1991; Narayan et al. 1992; Abbott et al. 2017c*], a kilonova [*Metzger 2017*], and the afterglow emission powered by a newly formed relativistic jet [*Sari et al. 1998*]. Since these different phenomena manifest on very different timescales, we first describe the observational strategy that TAP will employ to identify and characterize multi-wavelength counterparts to neutron star mergers, before discussing their expected rates.

The first potential signal, nearly coincident with the merger itself, will be a short GRB detected by the GTM. Given the large FoV of the GTM and the short time lag (2 s in the case of GW170817; *Abbott et al. 2017c, Goldstein et al. 2017*), on-board GTM detections will be entirely independent of signals from

ground-based GW detectors. GTM will monitor the sky in its 8 detectors searching for rate increases on timescales from ms to seconds in several energy channels, similar to previous instruments (e.g. BATSE, *Fermi*-GBM). When a rate increase is detected in at least 2 detectors, GTM will trigger, determine an onboard localization by using the relative rates in each detector compared to an onboard lookup table, and send down a sequence of localizations, and photon data in a window around the trigger. The WFI will immediately begin follow-up observations of the GTM localization, tiling if necessary.

Based on either a GW sky localization uploaded to the spacecraft or an on-board GTM trigger, TAP will immediately begin searching for an on-axis afterglow, as this component is expected to be quite bright but rapidly fading (time scale \sim minutes to hours). TAP will first slew to cover the localization with the WFI (utilizing multiple tiles if necessary). For small localizations ($< \sim 20 \text{ deg}^2$), the spacecraft will apply small offsets every $\sim 100 \text{ s}$ to also cover the region with the XRT and IRT.

If no counterpart is identified in these observations (e.g., an off-axis event), after $\sim 1 \text{ hour}$ TAP will shift focus to cover the localization with 300-s exposures with the IRT, to search for the associated kilonova (time scale \sim hours to days) and an off-axis afterglow with the XRT. The IRT will cover the error region twice to search for variability.

Even if no kilonova emission is detected in the IRT (e.g., very low ejecta mass), TAP will periodically monitor the localization with deep XRT exposures on time scales of weeks to months to search for off-axis afterglow emission. For reference, the X-ray counterpart of GW170817 peaked on a time scale of $\sim 200 \text{ d}$ [Troja et al. 2018, Nynka et al. 2018, Alexander et al. 2018].

Ground-based GW Network Counterpart Rates

We estimate the detection rates of gamma-ray, X-ray, and IR counterparts from GW detection from the GW network formed by the LIGO Hanford & Livingston, Virgo, KAGRA and LIGO-India detectors. **Table 3.3** shows the average GW sky map area, and duty cycle, obtained with 2, 3, 4 and 5 GW detectors [Leo Singer, private communication]. All of the sky maps can be observed with the GTM and at most a few pointings of the WFI; sky map areas of 30 deg^2 and smaller can also be observed with the XRT and IRT by tiling, using their respective 0.8 deg^2 and 1 deg^2 FoV to scan the area.

Table 3.3: *GW Network Sky Map Areas*

Number of GW detectors in operation	Duty Cycle	Average Sky Map Area within 90% CR (sq. deg)	Observing Instruments
2	14%	700	GTM, WFI
3	28%	100	GTM, WFI
4	34%	30	GTM, WFI, XRT, IRT
5	20%	17	GTM, WFI, XRT, IRT

Table 3.4: *GW Network Counterparts and associated rates measured by TAP.*

Counterpart Bandpass	Detector	Counterpart ¹	Enhanced BNS GW Horizon ²	Counterpart Detection Efficiency	Observation Time per Event	Counterpart Detection Rate (yr ⁻¹)
Gamma-ray	GTM	Prompt on-axis	485 Mpc	0.8	10 sec	20
Gamma-ray	GTM	Prompt off-axis	323 Mpc	0.01	10 sec	2
X-ray	WFI	Afterglow on-axis	485 Mpc	0.75	200 sec	20
X-ray	XRT	Afterglow on-axis	485 Mpc	0.9	1 hour	24
X-ray	XRT	Afterglow off-axis	323 Mpc	0.1	20 hour	7
Optical/IR	IRT	Afterglow on-axis	485 Mpc	0.7	6 hour	20
Optical/IR	IRT	Kilonova	323 Mpc	1	6 hour	70

1. An off-axis counterpart is assumed to have the luminosity associated with GW170817.
2. The GW horizon is enhanced for on-axis orientation by a peaking of the GW amplitude along the jet axis.

In **Table 3.4**, TAP counterpart detection rates are obtained in the following way. First, the nominal BNS horizon for LIGO in the late 2020s will be extended from the Advanced LIGO design sensitivity of 190 Mpc, to the LIGO A+ upgrade sensitivity of 323 Mpc (*LSC Instrument Whitepaper; URL#3*). A further enhanced BNS GW horizon occurs if the GW signal is on-axis which raises its amplitude by a factor of 1.5. The rate of BNS mergers and associated counterparts within that horizon volume is then calculated assuming a volumetric rate of BNS mergers of 1000 Gpc⁻³ yr⁻¹ (a horizon of 323 Mpc gives ~140 mergers/yr.).

The detection efficiency, and the detection rate, of the different counterparts are simulated by using the expected counterpart signal flux, and the detector sensitivities listed in **Table 4.1**. In the case of the off-axis gamma-ray, X-ray, and IR signals we use the fluxes obtained from the multi-wavelength counterpart study of GW170817, along with its observed distance of 40 Mpc, to find the detection efficiency, and associated counterpart detection rate within the enhanced GW horizon. In the case of the on-axis gamma-ray and X-ray counterparts, we use the set of prompt gamma-ray and afterglow X-ray fluxes with known redshift as measured by *Swift*, scaled to the enhanced GW horizons, and include a beaming factor of 0.06.

Finally, the observing time associated with the wide-field instruments (GTM, WFI) is short because the GTM has full-sky coverage, and only a few WFI pointings are necessary to cover even the largest GW sky map. For the narrow-field (0.8 & 1 deg² FoV) instruments (XRT & IRT), a weighted average of 37 pointings (after accounting for overlaps) will be necessary to tile the sky maps of **Table 3.3** for 4 or 5 GW detectors in operation; including the integration time in **Table 4.1** associated with the XRT and IRT sensitivities gives the total observing time per event. Including the detection efficiency and the number of

detections for each type of counterpart gives the total fraction of TAP time associated with the Ground-based GW Network (see **Fig. 1.3**).

3.3.2 LISA

LISA is expected to detect many mergers of SMBH binaries, which are also promising sources of electromagnetic emission in the X-ray band. Predicting rates of multimessenger observations of LISA SMBH systems is complicated by two aspects. First, the SMBH merger rate itself is still model-dependent [Klein *et al.* 2016]. Second, the processes that power the electromagnetic emission from an SMBH binary are complex and their details are still under active research [Bowen *et al.* 2018; D’Ascoli *et al.* 2018].

One can nevertheless take a fiducial SMBH merger rate and mass distribution, and construct a basic model of the X-ray emission using AGN observations and results from numerical simulations available to date. The electromagnetic emission from an SMBH binary approaching merger is generally expected to have two main features: a brightness that increases over time and a quasi-periodic modulation due to the dynamics of the gas being accreted on the two BHs [Haiman 2017]. Such a picture can be used to construct a full simulation of a population of SMBH binaries, taking into account how LISA would observe each system and how XRT could be used to search for the modulated X-ray counterpart while LISA is still observing the inspiraling system [Dal Canton *et al.* 2019]. Assuming a base Eddington luminosity with a modulation arising purely from the orbital Doppler boosting of the accreted gas around each BH, and a fiducial LISA detection rate of 10 yr^{-1} SMBH systems at redshifts closer than 3.5, the simulation finds a XRT detection rate of approximately 1 yr^{-1} . Most of these detections will happen in the last week of the SMBH inspiral, enabling an early alert of the merger with a precise sky localization, and providing observational data about the physics of gas accretion on a binary BH. The simulation in [Dal Canton *et al.* 2019] also takes into account the required TAP observing time, and enables an initial optimization of the TAP observing schedule with respect to detection rate and observing time. The best schedule found consists in waiting for the LISA sky localization to be more precise than $\sim 20 \text{ deg}^2$ before beginning the TAP observation. In this way, a TAP allocation of about 10% of the total observing time appears to be sufficient to achieve the 1 yr^{-1} detection rate.

Some of the assumptions and simplifications in [Dal Canton *et al.* 2019] are conservative, and relaxing them may lead to higher detection rates. If the orbital dynamics modulates the accretion rate itself, which is suggested in [Kelley *et al.* 2018], the X-ray signal would have an even stronger quasi-periodic modulation, making the systems easier to detect. It might also be possible to identify the X-ray source through post-merger features in the lightcurve, which are not considered in [Dal Canton *et al.* 2019]. Improvements in the LISA data analysis, or large component spins in SMBH systems, might also make the early sky localization of the GW signal more precise than what has been considered so far, allowing TAP to point to the correct region of the sky for a longer time. Finally, the process of observing an inspiraling LISA SMBH source with limited-field electromagnetic telescopes will be optimized further in future studies and might lead to a significant increase in detection efficiency and/or reduction of the required observing time.

3.3.3 Pulsar Timing Array (PTA)

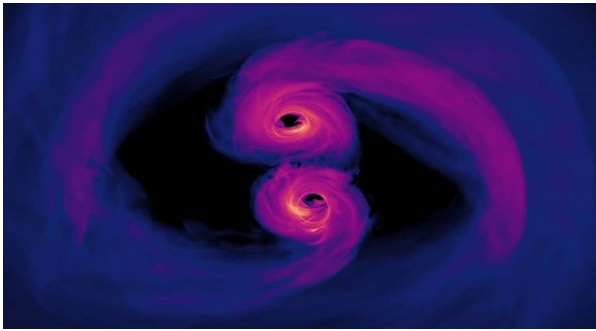


Figure 3.1: *Accreting SMBHB systems are compelling candidates for detection in gravitational waves with PTA and X-rays with TAP-WFI. Computer simulations of an accreting SMBHB system provide estimates of luminosity and evolution of these systems.*

Based on the steadily improving sensitivity of pulsar timing arrays and the expected occupation fraction of SMBH binaries in the local Universe (**Fig. 3.1**), by the year 2030 we expect at least a handful of binary SMBHs to be detected and individually resolved by PTAs (*Mingarelli et al. 2017*). Already, the North American Nanohertz Observatory for Gravitational Waves (NANOGrav) has a (sky dependent) sensitivity to a binary of chirp mass of $10^9 M_{\odot}$ out to a distance of 190 Mpc, and a chirp mass of $10^{10} M_{\odot}$ out to 8.9 Gpc (*Vigeland et al., submitted*). The high masses of, and relatively small distances to such systems suggests they will be both bright and also rare, making them ideal sources for detection with the WFI. Simulations of modulated X-ray emission from these sources, with period ~ 1 year, lead us to expect several TAP observations of EM counterparts to PTA sources over the course of the mission [*Schnittman 2014*].

The observing strategy for searching for EM counterparts to PTA sources is quite different to that described above for LISA counterparts. In particular, these sources will typically be slowly varying (orbital periods of weeks-to-years, expected flux modulations at $\sim 10\%$ level in X-rays) and long-lived, so should not be thought of as “events” but rather a catalog of candidates, with confidence and source properties evolving throughout the TAP mission. Initial estimates suggest that TAP will be able to detect roughly 10-20 of these binary sources over its mission lifetime, most of which would be beyond the range of initial PTA surveys [*Schnittman 2014*]. Promising periodic sources identified in the WFI sky survey can be observed in greater detail, with both the XRT or other observatories across the EM band. Again, because these sources are bright and long-lived, they are ideal for detailed multi-wavelength follow-up.

Eventually, PTA detections will provide a direct measurement of the GW phase and frequency of a binary, which is among the more critical parameters in direct counterpart identification. PTA measurements will still have degeneracies in mass, distance, and eccentricity. Identifying the host galaxy of such a system can break the mass/distance degeneracy through a redshift measurement, and thus allow a precision mass measurement for the binary that can be directly compared to host galaxy properties. The identification of clear counterpart signatures at any waveband will both contribute to studying these objects as multi-messenger targets, and serve as a “Rosetta Stone,” allowing existing and future surveys to identify and study a vast population of binary systems previously unidentified as SMBHBs.

3.4 Time-Domain Astronomy

TAP's versatile instrument suite and operations also make it an excellent facility for a wide variety of transient and variable source discovery and follow-up observations as outlined in §2.2. In the following section, we describe the basis for our source rate estimates (**Table 3.2**) and how they might piggyback upon our gravitational wave counterpart programs or community driven science observations.

To calculate the source rates for the WFI, XRT, and IRT, we assumed a simplified concept of operations. We assume that the WFI will survey almost all the unconstrained (~85%) sky weekly with approximately uniform exposures. The remaining 15% of the sky includes the observing (Sun/Earth/Moon) constraints. The exposures and corresponding sensitivities used in the estimates of source rates are summarized in **Table 3.5**.

Using these average exposure times, we interpolated the sensitivity in the WFI and XRT using our average sensitivity curves for a power law spectrum with photon index of 2 and absorption of $1e21 \text{ cm}^{-2}$.

For the XRT/IRT, we assume they will not observe the entire sky, but rather be co-pointed at the center of the 25 WFI fields. We do not assume they will be toggled to build up larger medium-deep fields, but that is a potential trade study.

Table 3.5: Average exposure and sensitivity for WFI and XRT fields during survey, follow-up, and TOO observations. The majority of XRT pointings will vary daily.

	Daily	Weekly	Monthly
Average WFI Exposure (ks)	2.7	19.3	82.8
WFI Sensitivity ($\text{erg cm}^{-2} \text{ s}^{-1}$)	1.7×10^{-11}	5.3×10^{-12}	2.1×10^{-12}
XRT Sensitivity ($\text{erg cm}^{-2} \text{ s}^{-1}$)	4×10^{-15}	--	--

3.4.1 Gamma-ray Bursts

The rate and population distributions of long duration GRBs was derived from an intrinsic sample developed for evaluation of the *Swift*-BAT sample in Lien et al. (2014). We built a simulation tool for the WFI including GRB prompt emission and afterglows derived from *Swift*-BAT and -XRT data. The WFI simulator includes realistic backgrounds, instrument parameters, and observing sequences. The simulation includes both paths to GRB detection: 1) GTM detection followed by WFI tiling in search of the afterglow and 2) detection by the WFI of the prompt emission and/or ongoing afterglow during the survey and other targeted observations. Detections with the WFI will be followed by IRT/XRT observations to determine spectra, light curves, and accurate positions.

TAP has a higher portion of high-redshift GRBs than current or previous instruments because of several factors (**Fig. 3.2**):

- Soft energy bandpass (0.3-5 keV) includes both the prompt emission and afterglow. Given that there are more photons and the spectral peak is shifted to lower energies, GRBs are bright in this band for thousands of seconds.

- With its high sensitivity and broad wavelength coverage including the NIR, the IRT will be very efficient at determining redshifts for GRBs, compared to for instance *Swift*-UVOT. This is especially the case for those GRBs that are heavily extinguished or at high z . Prompt autonomous low-resolution spectroscopy will provide indication within minutes knowledge of whether or not a GRB is at high- z . For GRBs at redshifts > 4 , the IRT will determine the redshift with an efficiency of $\sim 90\%$ (McQuinn 2008) and a relative accuracy of $\sim 5\%$. Large ground-based telescopes will rapidly be informed of which GRBs are available for high-resolution spectroscopy.
- TAP's L2 orbit provides an instantaneous field of regard 25-50% larger than instruments in a low Earth orbit (depending on the instrument and its Sun/Earth constraints). The larger field of regard is a larger field of view for the GTM, and allows for faster follow-up with the WFI, XRT, and IRT before the sources fade away. This boosts the GRB rate, especially for follow-up of external triggers.

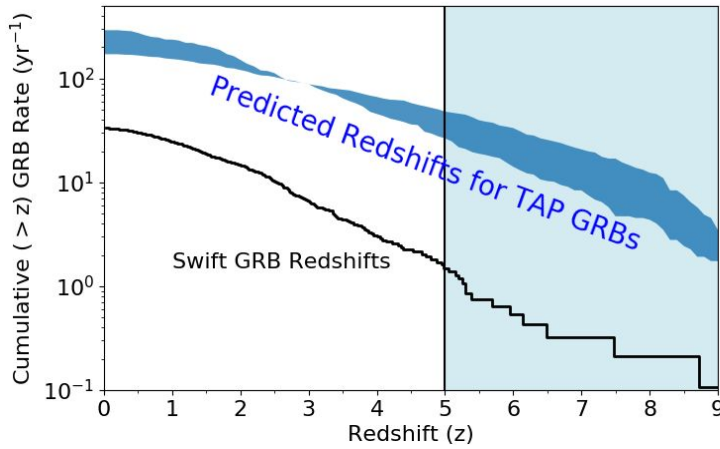


Figure 3.2: Simulated distribution of TAP long duration GRB redshifts relative to Swift GRB measured redshifts. TAP's higher rate of GRBs and higher efficiency at redshift measurements make it a very efficient facility for selecting candidate sources to be probes of the high- z Universe.

3.4.2 Tidal Disruption Events (TDEs)

Discovery and follow-up of TDEs in the soft X-ray band promises to substantially increase the sample size, providing population level analyses of this interesting source class. The known TDEs can be separated into the highly luminous jetted events, and the non-jetted events, where presumably the jet is pointed away from us. We calculate the rate of TDEs by assuming their specific rate as $10^{-4} \text{ yr}^{-1} \text{ galaxy}^{-1}$ [van Velzen et al. 2018], in galaxies with 10^6 - $10^8 M_{\odot}$ SMBHs, which a density of 10^{-2} Mpc^{-3} .

Non-jetted TDEs have thermal spectral with blackbody temperatures of $kT=0.05 \text{ keV}$, and bolometric luminosities of $10^{44} \text{ erg s}^{-1}$. Converting bolometric to the WFI (0.3-5 keV) and XRT (0.4-6 keV) bandpasses, we calculate the redshift from the luminosity distance out to which these sources could be detected, and convert that to a comoving distance and volume, multiplied by the volumetric rate and galaxy density and the fraction of sky observed with that sensitivity (85%). The resulting source rates are given in **Table 3.2**.

Jetted TDEs have non-thermal spectra with a photon index of 2, average absorption of 10^{21} cm^2 , and bolometric luminosities of $10^{47} \text{ erg s}^{-1}$. The jet is pointed towards Earth for only $\sim 10\%$ of these events. Similarly to accounting for the non-jetted events, the bandpass is converted, and the volume calculated for detecting these events out to their luminosities, and then multiplied by 0.1 times their rates. The resulting source rates are given in **Table 3.2**.

3.4.3 Supernovae

Ground-based surveys in the 2020s (e.g., LSST) will discover many millions of new SNe, making the challenge not of detection, but of distilling the list down to those that are interesting to follow up. TAP will be an excellent resource for rapid follow-up of unusual SNe, as well as monitoring their evolution over the months afterwards.

One topic where TAP will provide unique discovery space is in ccSNe Shock Breakouts. These rare short-lived (hundreds of seconds) transients provide not only the precise time of the SN, but important physics about the initial explosions. They will be detected by WFI and XRT during survey pointings longer than the transient duration, they do not require all-sky survey, or any special modes of operation.

Swift-XRT serendipitously detected SN2008D as a $\sim 400 \text{ s}$ transient soft X-ray source with a flux of $\sim 4.5 \times 10^{-11} \text{ ergs cm}^{-2} \text{ s}^{-1}$ at a distance of 27 Mpc and a luminosity of $6 \times 10^{43} \text{ erg s}^{-1}$. The unique and extremely low probability detection of such a source once over the 14 year *Swift* mission, demonstrates the power of a soft X-ray mission with a much larger FoV and/or sensitivity.

In 400 s of exposure, the WFI has a sensitivity of $\sim 5.5 \times 10^{-11} \text{ ergs cm}^{-2} \text{ s}^{-1}$, and the TAP-XRT has a sensitivity of $2 \times 10^{-14} \text{ ergs cm}^{-2} \text{ s}^{-1}$. Therefore, SN2008D would have been detectable out to 74 Mpc (WFI) and 1.9 Gpc (XRT). Given a rate of SN Ibc rate from Li et al. (2011) of $2.58 \times 10^{-5} \text{ SN Mpc}^{-3} \text{ yr}^{-1}$, a conversion from the observed *Swift*-XRT energy band of 0.3-10 keV to the WFI/XRT bandpasses using the *Swift*-XRT spectrum, and scaling for FoV. The resulting source rates are given in **Table 3.2**.

3.4.4 AGN and Blazars

Active galaxies are the most prolific of the extragalactic X-ray sources. They vary on all timescales and randomly go into outburst. TAP will be ideally suited to monitor their behavior in the X-ray band across the whole (non-constrained) sky, providing triggers for follow-up observations when source are in elevated states, much as Fermi-LAT does in the high-energy gamma-ray band for blazars.

To estimate the WFI/XRT detection rate for the non-blazar AGN, we used the 0.5-7 keV luminosity function from Povi et al. [2013]. After converting to the WFI and XRT bandpasses, we calculated the distance out to to which each of the luminosity functions bins could be above the WFI/XRT sensitivity limit for a similar absorbed power law spectrum. We turned that distance into a co-moving volume and

integrated over the luminosity function for daily and weekly exposures as described in **Table 3.5**. The resulting source rates are given in **Table 3.2**.

To estimate the source rate for Blazars, we adopted a similar approach, but directly use the log N - log S distribution from Padovani et al. [2007]. After converting the bandpass and determining the sensitivity limit for WFI/XRT, we integrated the distribution above that threshold and scaled by the FoVs. The resulting source rates are given in **Table 3.2**.

3.4.5 Novae Thermonuclear Flash

The peak luminosity of Galactic thermonuclear runaway novae flashes is $\sim 10^{38}$ erg s⁻¹, occur at a rate of 35 ± 11 yr⁻¹ [Shafter 1997], and lasts ~ 100 seconds. At the distance of the Galactic center (8 kpc), the flux would be 1.3×10^{-8} erg cm⁻² s⁻¹, which is well above the WFI and XRT sensitivity limits on 100 sec timescales. Therefore the sensitivity is not a limiting factor, but instead the rate is determined by the instruments' FoV. Therefore the WFI should detect ~ 1 yr⁻¹, and the probability of the XRT detecting one is extremely low. The WFI/XRT will certainly be capable of following up both X-ray and optical discovered novae as they are in outburst. The source rates are given in **Table 3.2**.

3.4.6 Thermonuclear Bursts

Previous wide-field X-ray missions such as BeppoSAX and RXTE detected populations of thermonuclear bursts [Cornelisse et al. 2003, Keek et al. 2010]. These short-lived (few hundred second) transients are bright, well above the thresholds of WFI/XRT. Therefore we scale the rates by FoV to calculate the values given in **Table 3.2**.

3.4.7 Neutrino Counterparts

The 2017 discovery of a gamma-ray flare associated with an IceCube neutrino event revealed the blazar TXS 0506+056 as the first extragalactic VHE neutrino point source (SN1987A was extragalactic as well, but its neutrinos are thermal in nature and associated with core collapse of a massive star). Follow-up in archival IceCube data revealed earlier neutrino events from the same source (Aartsen et al. 2018), which suggests that gamma-ray monitoring could reveal further coincidence, and establish stronger constraints on the physics at work in these sites. The AGILE team searched for transient gamma ray counterparts to IceCube HESE/EHE events (Lucarelli et al. 2019) and reported three candidate gamma sources (emitting above 100 MeV) out of 11 IceCube neutrino targets (one of these three is the previously established source XS 0506+056). While there is insufficient data to allow for reliable rate estimates, these recent observations suggest that TAP will enter a promising discovery arena in the neutrino sector. To date we have only one secure link between a UHE neutrino and a flaring blazar, but such correlated emission is the natural signature of particle acceleration sites that are dominated by hadronic process. True MMA events involving neutrinos and gamma-rays and added X-ray and IR information from TAP would revolutionize this field. The increased neutrino detection rates from IceCube-Gen2 will lead to increased opportunities for TAP and other future wide-field of view transient response instruments.

3.4.8 Exoplanets

As stated earlier, the breadth of TAP instrumentation, and its rapid response capability, allows for consideration of applications beyond transient astrophysics. The TAP IRT aperture size and modern low-noise detectors along with the high pointing stability of the observatory will make it a capable instrument that can contribute key measurements for exoplanet characterization. Conservatively assuming TAP IRT will meet the photometric precision achievable with *Spitzer* (~ 300 ppm), a comparably sized IR telescope, we investigated potential exoplanet science cases for the mission. Spectroscopic observations of exoplanets during transit provide key information on their atmospheric properties and allow comparative exoplanet science to constrain formation pathways and compositions. The spectroscopic capabilities of the IRT can provide low-resolution exoplanet spectra spanning a wide wavelength range covering key atmospheric absorption features such as Na, K, H₂O, CO₂, and CH₄. Using the simulated planet yield expected from the TESS survey to estimate the number of planets amenable to transit spectroscopy using the IRT spectrograph, TAP could detect atmospheric features in ~ 300 TESS-detected planets orbiting stars 8-12 magnitude (1-20 sec integrations) ranging in size from ~ 2 Earth radii to >1 Jupiter radius. By observing several transits of planets in resonant multi-planet systems over long time baselines using multi-band photometry, TAP IRT will also be able to measure transit-timing-variations (TTVs) and provide access to exoplanet masses via dynamical modeling. TTV measurements focusing on a carefully selected sample of multi-planet systems would provide new points on the exoplanet mass-radius diagram for deeper insight into the bulk densities and compositional diversity of exoplanets. TAP IRT will also be sensitive to the thermal emission from hot, giant planets on short period orbits, allowing the measurement of phase curves and secondary eclipses. Phase curve and secondary eclipse measurements provide access to the temperature on the dayside and nightside of the planet and allow the thermal structure of the atmosphere to be inferred. In addition, the very broad, simultaneous wavelength coverage of the TAP IRT, along with simultaneous observations of the same field with the XRT, will allow access to not only exoplanet transits but also host star activity (spot variability, energetic flares), a key factor in understanding the impact of the host star on exoplanet atmospheres and ultimately planet habitability. We estimate that an exoplanet follow-up program targeting dozens of planets for atmospheric spectroscopy, ~ 10 systems for TTV mass measurements, and ~ 5 hot Jupiters for phase curve/secondary eclipse measurements could be undertaken using $\leq 5\%$ of the total TAP observing time. This program would be designed to complement other facilities performing exoplanet measurements in the era of TAP (e.g. JWST) to maximize the scientific return from the mission.

4. Instrumentation Payload

The TAP instrument suite is comprised of the WFI, XRT, IRT, and the GTM, providing a system that promptly provides arcmin to arcsec positions of transients and EM counterparts to events detected by the Ground-based GW Network (**Table 4.1** lists the basic requirements). WFI, IRT, and XRT images of the sky are scanned by software in the on-board computer to locate new and existing sources during both Survey and Target of Opportunity (TOO) operations. TAP rapidly alerts ground- and space-based facilities to the detection of new sources, so that they can perform follow-up observations in all wavebands.

TAP will stare at ~50 regions of the sky per day, searching for new transients and monitoring known sources for changes in their count rates. In response to a WFI trigger, TAP continues observing the newly found transient source by slewing to that location so the XRT & IRT can get better localizations and measure light curves and spectra.

Table 4.1: *TAP instrument parameter requirements. [1] For GTM this is a localization metric, not a PSF. [2] Sensitivity of the trigger in the 50-300 keV band.*

Parameter	WFI	XRT	IRT	GTM
FoV	36.2x36.2° (0.4 sr)	1° dia	1x1° (sq)	4 π sr
Aperture Size	35x35 cm (each module)	130 cm dia; fl=500 cm	70 cm dia	20 cm each det
PSF/FWHM	9 arcmin	5 arcsec HPD	0.22 arcsec	20° radius[1]
Energy Range	0.4 - 5 keV	0.2 - 10 keV	0.4 - 2.5 μm	10 keV - 1 MeV
Sensitivity	2x10 ⁻¹¹ erg/sec cm ² (2 ks)	4.8x10 ⁻¹⁵ erg/sec cm ² (2 ks)	23 mag (300 s)	0.9 ph/cm ² /s[2]
Mass (CBE/MEV)	159 / 207 kg	294 / 382 kg	135 / 176 kg	53 / 69 kg
Power (CBE/MEV)	276 / 359 W	370 / 481 W	119 / 155 W	48 / 63 W
Data (CBE/MEV)	5 / 6.5 GB/day	0.3 / 0.4 GB/day	0.8 / 1.1 GB/day	0.15 / 0.2 GB/day
TRL	6	5 (6 by 2020)	6	6

Triggers can also be generated directly by XRT and IRT transients. TAP uses the low-latency continuously available NASA NEN and commercial ground station command/data links and a fast-slewing spacecraft to upload TOO locations, and send the positions, images, and light curves to the ground (and then out to the world via the GCN).

4.1 Wide-Field Imager (WFI)

- Large FoV (36.2 x 36.2deg, 0.4 sr) to detect GW counterparts from 2, 3, 4 or 5 GW detectors.
- High sensitivity to detect a wide variety of transients, & frequent surveys of the X-ray sky.
- 1.5 arcmin location accuracy is well matched to space-flight and ground-based follow-up instruments' FoVs.
- Commercially available multi-channel optics (MCOs) image a large FoV with constant effective area.
- Focusing optics provide >10 times higher sensitivity than previous missions (MAXI, RXTE-ASM).

Sensitivity: Each WFI telescope has MCOs to produce an X-ray image on the detector plane, and CCDs to detect X-ray photons. A preliminary trade study of FoV vs. location accuracy vs. cost identified a design with a 45-cm focal length MCO array (34x34 cm) and a 3x3 array of 5x5 cm CCDs that yields an optimum number of transients, coverage of the LIGO/Virgo sky error region, and sufficient location accuracy. This design yields a 0.4 sr FoV (for the 4 modules) with a point-spread function (PSF) of 7 arcmin full-width half-maximum (FWHM) and a centroiding accuracy of ~1 arcmin at threshold (**Fig. 4.1**). The sensitivity is 2.6x10⁻¹⁰ ergs s⁻¹ cm⁻² for a 40-sec transient in the 0.3-5 keV band and 2x10⁻¹¹ ergs s⁻¹ cm⁻² in 2 ks. Sensitivity estimation used ray tracing to measure the effective area, laboratory

measurements of the MCO (throughput efficiency and FWHM of the PSF), and a background based on a power-law with an energy index of 0.4 to represent the cosmic X-ray background and a thermal model for the Galactic X-ray background.

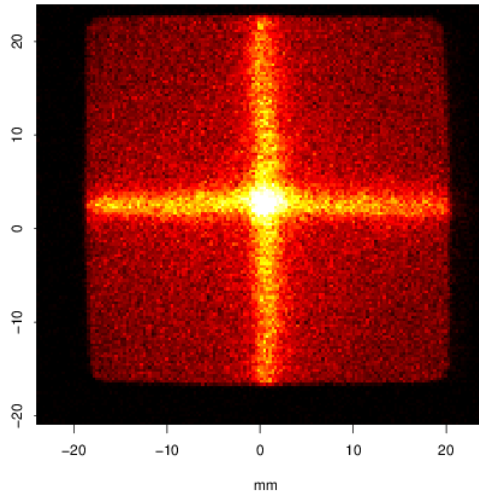


Figure 4.1: PSF of MCO measured at X-ray beamline by Co-I Willingale at U. Leicester, $FWHM \approx 7$ arcmin.

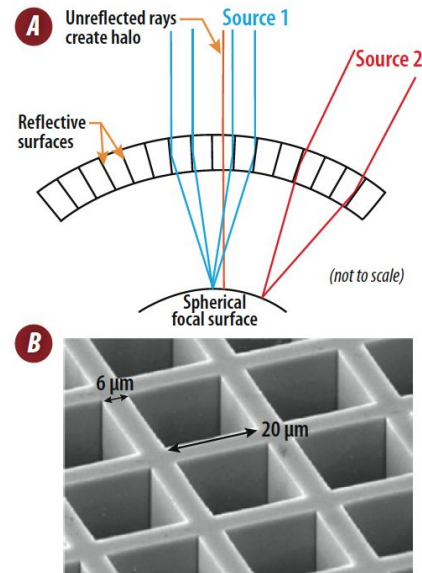


Figure 4.2: (A) Diagram of the focusing aspects of the MCO, and (B) a photo-micrograph of a few pores in an MCO (Ir coating and OBF not shown).

Micro-Channel Optics: The MCOs are the key to the WFI design. These optics, originally proposed by *Angel (1979)*, mimic the eye of a lobster, providing constant imaging performance and effective area across the entire FoV. The optic consists of microscopic square channels extending radially from a spherical surface manufactured in glass (**Fig 4.2A**). Approximately 25% of incident X-rays are reflected twice, off two adjacent sides of the channels, forming a true image at a distance half the radius of curvature (RoC) from the optical surface while approximately 50% are reflected off only one surface and form a cross-like pattern. The remaining 25% pass straight through the channels without reflection forming a diffuse halo around the image. The inner surfaces of each channel are coated with iridium for improved X-ray reflectivity (50-80%). With an 8x8 array of MCO tiles, each $40 \times 40 \text{ mm}^2$, and an RoC of 900 mm (focal length 450 mm) the FoV is $18.6 \times 18.6^\circ$ (0.1 sr) each. The net effective area at 1 keV (including CCD and filters) is 2.4 cm^2 for the central spot focus portion of the PSF. And for spectral and temporal measurements of bright sources, the effective area of the cross-arms (4.5 cm^2) can be included in the analysis. MCOs have been under development at the University of Leicester and were used in the Mercury Imaging X-ray Spectrometer instruments (MIXS-C and MIXS-T) on BepiColombo [*Fraser 2010*] that was launched 20th October 2018. The MIXS MCOs passed all of the environmental tests, vibration, thermal vacuum, acoustic, launch depressurization, and a 1-atm static differential test, and the TAP MCOs are at TRL 6.

CCD Detectors: WFI's CCDs and front-end electronics, that will be designed and built by the MIT Lincoln Laboratory and MIT, respectively, detect X-ray photons and record the detection location and

energy. Each focal plane assembly (FPA) is composed of a 3x3 array of 5x5cm CCDs that operate at -60°C . The 9 CCDs in the FPA are tip/tilted to approximate the spherical focal surface of the MCOs. The energy resolution is $<200\text{ eV FWHM}$. The CCDs are cooled to -60°C by heat pipes and passive radiators. The CCD are derived from the TESS design (but without the frame-store capability). The out-of-time readout fraction is $<7\%$ for the shortest integration time of 2 sec. The CCDs are TRL 6.

On-Board Data Processing: The individual X-ray events readout from the CCDs are proceed on-board to find new and known sources. The first steps is to find the peaks in the image domain. This is done for each CCD. Five 2-sec integrations are stacked and scanned for peaks in 2 to 3 energy bands (0.3-2, 2-5, and 0.3-5 keV). The sources found are checked against an on-board catalog (e.g., RASS augmented with new sources). New sources are immediately reported to the ground. Further stacking to 20, 40, 80, ..., 640 sec are made and searched for new and known sources. This covers the real-time detection of transients. After the full event-by-event data is transmitted to the ground, more sensitive analysis will confirm and improve the real-time detections and find other fainter transients.

4.2 Infrared Telescope (IRT)

- Large FoV ($1\times 1^{\circ}$) and high sensitivity to detect GW IR counterparts (kilonova) and a large number of transients.
- Arcsecond location accuracy (plate scale is 0.9 arcsec/pixel).
- Spectroscopic redshift determination to 5% over $4 < z < 16$.

The IRT will localize sources identified by the WFI to within 0.5 arcsec relative to nearby stars, perform 4-band photometry and determine the redshift for high- z GRBs (and other targets), and search for the potential kilonova of a NS-NS merger (identified by a GW detection.) The IRT is a 70-cm telescope with two instrument channels (**Fig 4.3**): 1) a wide-field imager that uses dichroics to obtain images in three bands simultaneously onto three IR & one visible detectors, and 2) a low-resolution ($\lambda/\Delta\lambda \sim 30$) slit spectrometer (slit width ~ 3 arcsec). The spectrum is projected onto a small strip of one of the detectors. The overall instrument bandpass is $0.4\text{-}2.5\ \mu\text{m}$ (with possible extensions to $0.3\ \mu\text{m}$ and to $3\ \mu\text{m}$ to be investigated), divided into 4 separate imaging bands. Guide stars extracted from the IRT images provide an overall pointing stability of 0.35 arcsec.

The telescope is a Korsch 3-mirror anastigmat that provides well-corrected images over a wide FoV and an accessible exit pupil. The fold mirror behind the primary is mounted on a fast steering mechanism to provide the fine pointing stability requirement. A pickoff mirror and slit at the Cassegrain focus directs light into the spectrometer, while the offset imaging field continues to the tertiary mirror and aft-optics assembly. The Optical Telescope Assembly (OTA, the tube) is cooled to 210 K by passive radiators. An aft-optics assembly contains the imager optics, spectrometer, and detector. The imager optics consists of dichroics that define the three imaging bands and fold mirrors that direct the three images onto the different detectors. The IRT focal plane, cooled by a cryocooler to $\sim 90\text{ K}$, consists of 3 Teledyne Imaging Sensors 4Kx4K sensor chip assemblies (SCA) (3 H4RGs & 1 HiViSi). These SCAs were developed for the WFIRST program, for which the flight devices have been qualified.

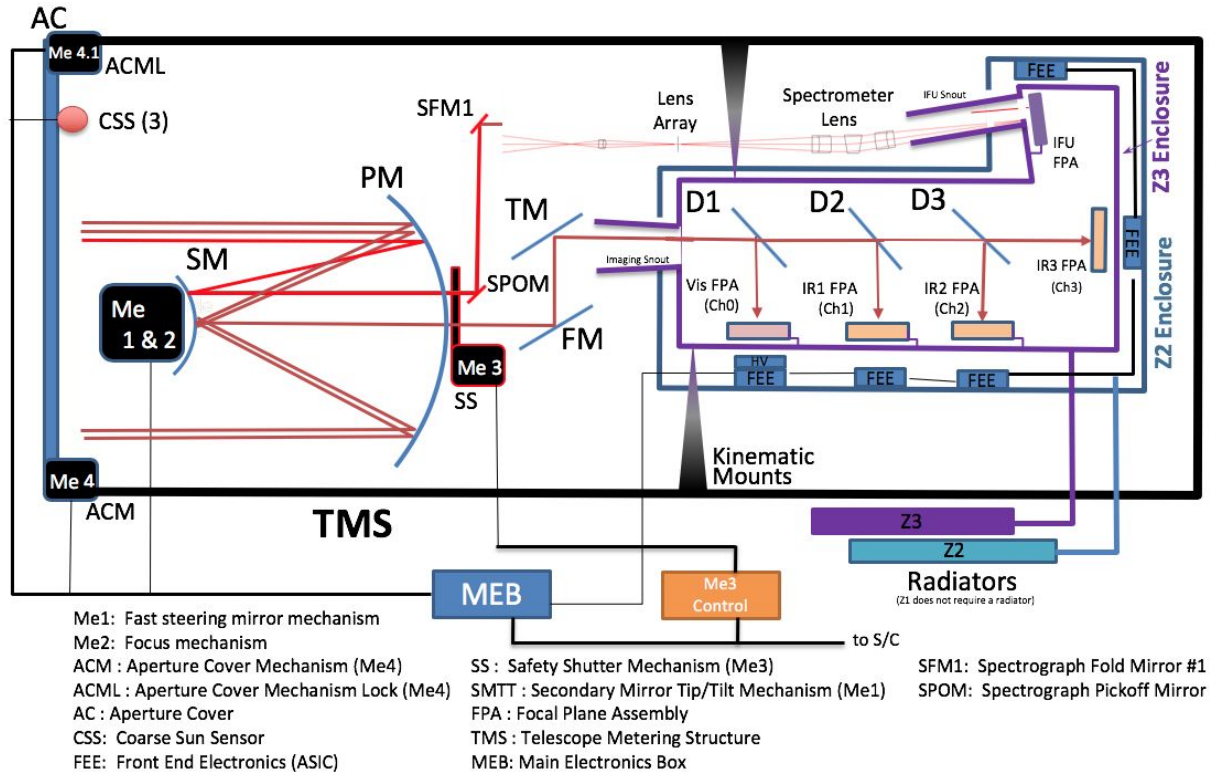


Figure 4.3: Schematic of the IRT optics and detectors for the 4 imaging bands and the one spectroscopy channel.

Sensitivity: To determine the IRT response to a given flux, we computed the total signal from the 70 cm aperture, and estimated the 5-sigma limiting sensitivity assuming a simple 2x2 pixel extraction. The PSF was computed including diffraction and MEV pointing jitter, charge diffusion, and budgeted wavefront error. The ensquared energy in 2x2 pixels was 71.9%, 69.2%, and 60.3% for Bands 1, 2, and 3. Backgrounds included zodiacal light at 4 times the North Ecliptic Pole value (2-3 times NEP is typical for most TAP pointings), MEV for dark current, read-noise, and telescope thermal emission. The effective read-noise was computed from the MEV CDS value and scaled for non-destructive readouts spaced uniformly throughout the exposure. The flux limit for a flat spectrum source in a 300 second exposure used to locate a kilonova is $AB \approx 23$ for all 4 bands.

To achieve the full performance and sensitivity of the diffraction-limited telescope (0.5 arcsec FWHM at $1.5 \mu\text{m}$), a fast steering mirror (FSM) is used to remove the S/C pitch and yaw jitter. The instrument components, all commercially available including detectors (Teledyne), telescope (L3Com), and aft optics, are TRL ≥ 6 .

4.3 X-ray Telescope (XRT)

- Large FoV (1° dia) for finer location of transients and deep surveys of small regions of the sky
- High sensitivity (5×10^{-15} erg $\text{cm}^{-2} \text{sec}^{-1}$ in 2000 sec & 7×10^{-14} in 100 sec).
- 2 arcsec location accuracy.

The XRT (**Fig. 4.4**) (McClelland *et al.*, 2017) provides ~ 2 arcsec source localization capability for all TOO targets, with much deeper sensitivity than the WFIs (4.8×10^{-15} erg/ cm^2/s in 2 ks), over a 1 deg diameter FoV. The large XRT FoV means that it can be used to search for X-ray counterparts to GW events, as well as function in a survey mode, probing deeply for transient sources. And using the XRT to improve on the WFI localizations will enable an additional set of ground- and space-based follow-up observers, and monitor the afterglow with much higher sensitivity.

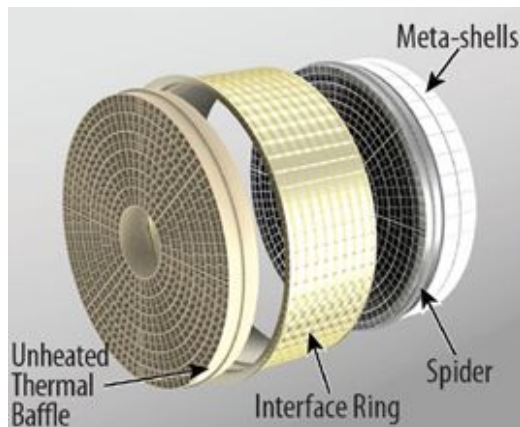


Figure 4.4: XRT mirror assembly; the focal length is 500 cm. (The focal plane array of detector is not shown, but is the common design using CCDs.)

Detector: The detector assembly (TRL 6) is based on CCD chips produced by MIT/LL. The focal plane array will be 100×100 mm of CCDs (2×2 array) with $45 \mu\text{m}$ 3×3 binned pixels ($1.8''/\text{pix}$). These chips are back-illuminated to achieve the best low energy response.

Tube: The telescope tube (TRL 7) is made of composite with an aluminum liner to prevent outgassing. The telescope assembly consists of three components: a mirror assembly, a detector assembly, and a telescope tube that mechanically connects the two.

Mirror: The mirror assembly consists of a large number of single crystal silicon mirrors, each of which is approximately $100 \text{mm} \times 100 \text{mm} \times 0.4 \text{mm}$, resulting in a maximum diameter of 1.3m. The mirrors are individually polished using a process that has been recently developed at GSFC [Zhang 2018], and coated with 20 nm of iridium to enhance their X-ray reflectivity. They are assembled together with silicon spacers and adhesive. As of December 2018, this mirror technology is at TRL 5, and a NASA-funded TRL-raising program is underway. An engineering test model has been constructed and vibrated to the level of GEVS EELV. Mirrors meeting TAP quality requirements have been made repeatedly, demonstrating the robustness of the process. The TRL-raising program (to TRL 6) will be completed in December 2020 (see §7).

4.4 Gamma-ray Transient Monitor (GTM)

- 4π sr FoV, $<20^\circ$ radius localizations; provides gamma-ray burst coincidences with GW events.
- Design based on the *Fermi*-GBM, which has been operating for 10+ years; TRL ≥ 7 .

The GTM provides all-sky detection of GRBs. In particular, it can detect simultaneous gamma-ray signals associated with NS-NS or NS-BH mergers detected by the Ground-based GW Network, including on-axis events as well as some off-axis events. The off-axis NS-NS merger GW170817 produced a short GRB that was detected by *Fermi*-GBM [*Abbott et al. 2017c*].

Detectors: The GTM consists of 8 detectors mounted on the spacecraft and instrument section such that there is one detector pointed along the directions of the faces of an octahedron (e.g. CGRO-BATSE), or if that is not possible for all 8 directions then an architecture more like *Fermi*-GBM. Both are tried and true approaches. Each detector is a 20 cm diameter by 1.27 cm thick disk of NaI(Tl) crystals that converts photons from 10 keV to 1 MeV into scintillation light. The crystals are housed in an aluminum enclosure and view the sky through a Beryllium window. The crystals are wrapped in a diffusively reflective material and the light escapes the crystal via one of the large faces via a quartz window which is transparent to the 415 nm scintillation light. This scintillation light is detected by light collecting devices such as a photomultiplier tube (PMT) or arrays of Silicon photomultipliers (SiPMs). The PMTs have the advantage of very high TRL (7 or above) but are large, massive, and require high voltage. SiPMs are solid state devices with low mass and volume and do not require high voltage but have lower TRL (6 or less). Several missions are in development which will fly large arrays of SiPMs in the next few years (e.g. BurstCube, GlowBug) which will bring the TRL of SiPMs in line with PMTs. A trade study will be undertaken during Phase A to determine if the readout will be based on SiPMs or PMTs.

Due to the geometry of the detectors, a gamma-ray source that is on axis produces more gamma-ray photon interactions in a detector than a source that is off-axis which provides directional capability if information from multiple detectors is combined (8 detectors will provide < 20 degree radius error regions, 90% inclusion). The detectors are pointed approximately evenly over a 4π hemisphere. The photon hits in each detector are continuously digitized and binned into light curves with various energy and time binnings to search for dramatic increases in count rates over the background indicative of a GRB. Two detectors are required to have rates above the threshold to be a valid trigger instead of one detector to eliminate the false positive triggers caused by cosmic ray hits. The trigger sensitivity is 0.9 ph/cm²/s for a 1 sec interval. The processing of the (a) event trigger, and (b) localization of the burst (via look-up tables) is done in the GTM Main Electronics Box (MEB). The light curves and localizations will be used to filter out events from the Sun and Cosmic Rays. Detections will be correlated with uploaded ground-produced GW network triggers, and also sent to the ground for correlation with sub-threshold GW triggers (and with other missions/instruments via distribution by GCN).

4.5 Descoped Instrument Performance and Rates

If, after further study, we find that we are getting close on any of the resource limits (cost, mass, power, telemetry), we have identified 4 descope options that can be exercised individually or in various combinations. There are no sensible descope options for the spacecraft bus, nor the concept of operations. The reductions in the detection rates from the descopes is shown in **Table 4.2** (see **Table 3.2** for the baseline detection rates and **Fig 9.1** for a schedule timeline).

WFI Module Count Descope: The reduction from 4 modules to 3 impacts (a) the Survey science (detection rates of transients; reduces the cadence by a factor of 4/3) and (b) the amount of tiling needed for L-V error region coverage on the 14% of LH-LL-V-K-I events that are 2-detector events (3-, 4-, & 5-detector events still only require one tiling to cover the full region). Further study is needed to see if a 3-inline arrangement of the 3 remaining modules is better than the L-shaped pattern. The $\sim 1^\circ$ overlap of the modules would be preserved. This is a \$16M reduction.

IRT Aperture Diameter Descope: The reduction of the aperture size from 70 to 60 cm has a modest reduction in the sensitivity by 0.2 mags (23 up to 22.8 mag) for a \$10M reduction in cost.

XRT Aperture Descope: The reduction in the XRT is done by removing the inner meta-shells while maintaining the outer diameter of the aperture, which has the most impact of cost and mass reduction. The reduction results in a 30% decrease in effective area and a cost savings of \$13M.

Non-Redundant GTM MEB Descope: All 4 instrument have redundant control/processing computers (MEBs), GTM is the least critical to the operations and science return to TAP (i.e. GTM provides temporal and spatial coincidence with the GW detections). Rolling back the Class B redundancy on this one instrument is acceptable risk. The cost savings would be \$~1.5M.

The net savings of the sum of these descopes, including their effects on the cost of Project Management, Systems Engineering, Mission Assurance, Science and Technology and Reserves is \$76M (see **Table 10.1**).

The effect of these descopes on the TAP science target rates is shown below in **Table 4.2**. A modest degradation of rates is seen for the source classes of GW counterparts, high-z GRBs, SN shock breakouts, and non-jettted tidal disruption events.

Table 4.2: *The decrease in the detection rates for each class of source object resulting from each of the 3 individual instrument descope options.*

Source Class	IRT Detections / yr Desclope / Baseline	XRT Detections / yr Desclope / Baseline	WFI Detections / yr Desclope / Baseline
GW NS-NS (on-axis)	15 / 20	34 / 24	20 / 20
GW NS-NS (off-axis)	55 / 70	5 / 7	--
GW SMBH-SMBH ($10^6 M_{\odot}$)	--	0.7 / 1	--
GW SMBH-SMBH ($10^9 M_{\odot}$)	--	--	Several / several (over 5 year mission)
High-z GRBs ($z > 5$)	20 / 22	--	19 / 25
ccSN shock breakout	--	13 / 19	0.7 / 1
Jetted TDEs	--	0.7 / 1	75 / 106
Non-jetted TDEs	--	32 / 48	0.7 / 1

4.6 TAP: a next generation transient observatory after *Swift*

The TAP mission provides roughly a factor of 10 improvement in instrument sensitivity and/or FoV over the highly successful *Swift* mission (see comparison in **Table 4.3**). And TAP retains the rapid response autonomy which is very important in transient astrophysics.

Table 4.3: *Comparison of TAP to Swift (the previous multi-EM band transient/survey mission).*

EM Band:	<i>Swift</i>	TAP
X-ray (wide)	BAT: Location Accuracy: < 3 arcmin $F_{\text{lim}}: 6 \times 10^{-10} \text{ erg cm}^{-2} \text{ s}^{-1}$ (2ks, 15-150 keV)	WFI: Location Accuracy: < 1.5 arcmin $F_{\text{lim}}: 2 \times 10^{-11} \text{ erg cm}^{-2} \text{ s}^{-1}$ (2 ks, 0.4-4 keV)
X-ray (narrow)	XRT: Location Accuracy: < 5 arcsec $F_{\text{lim}}: 1 \times 10^{-13} \text{ erg cm}^{-2} \text{ s}^{-1}$ (10 ks, 0.3-10 keV)	XRT: Location Accuracy: 2 arcsec $F_{\text{lim}}: 5 \times 10^{-15} \text{ erg cm}^{-2} \text{ s}^{-1}$ (2 ks, 0.2-10 keV)
UV - optical - IR	UVOT: Band: 0.16 - 0.7 microns $F_{\text{lim}}: 19.1 \text{ mag V band (300 s)}$	IRT: Band: 0.4 - 2.5 microns $F_{\text{lim}}: 23 \text{ mag (300 s)}$
gamma-ray	BAT: Location Accuracy: < 3 arcmin $F_{\text{lim}}: 3.0 \times 10^{-8} \text{ erg cm}^{-2} \text{ s}^{-1}$ (1 s)	GTM: Location Accuracy: < 20 deg $F_{\text{lim}}: 0.9 \text{ ph/cm}^2/\text{s}$ (1 s)

5. Mission Design

The TAP mission builds upon the multi-instrument and autonomy approach of *Swift* and uses a demonstrated spacecraft design with flight-proven components. TAP's dedicated low rate communications link and distribution of results to the community allows rapid follow-up of ground-initiated Targets of Opportunity.

The TAP mission design is well-suited to the instrument suite and science objectives and builds upon the successful mission design of *Swift*. The mission is accomplished with mature technology and without the need for complex deployments or in-space assembly. Stationing the observatory at the second Sun-Earth Libration Point (L2) provides high observing accessibility, no eclipses, and a low radiation dose. A Mission Design Laboratory (MDL) study was performed at GSFC from November 13 to 17, 2017. The output of that study is summarized below, with the full study being available in the Engineering Concept Definition Package. The expected performance of the system is summarized in **Table 3.1** (right-most column).

5.1 Launch and Early Operations

The TAP observatory is launched on an Expendable Launch Vehicle (ELV) and adopts the same launch profile planned for JWST. TAP fits well within an Atlas V 5m fairing, using an existing Payload Adapter Fitting (PAF D1666), while also being compatible with a launch by SpaceX Falcon-9. Following a coast phase, the upper Centaur stage propels TAP into a transfer trajectory to a large amplitude halo orbit around L2. On-board propulsion accommodates a 30 minute launch window and launch vehicle dispersion. TAP's propulsion system then makes two mid-course corrections before a final insertion into the L2 orbit shown in **Fig 5.1**. Station-keeping maneuvers are required about once every 3 months and consumables are sized to meet the 5-year mission lifetime and a 10 year design goal.

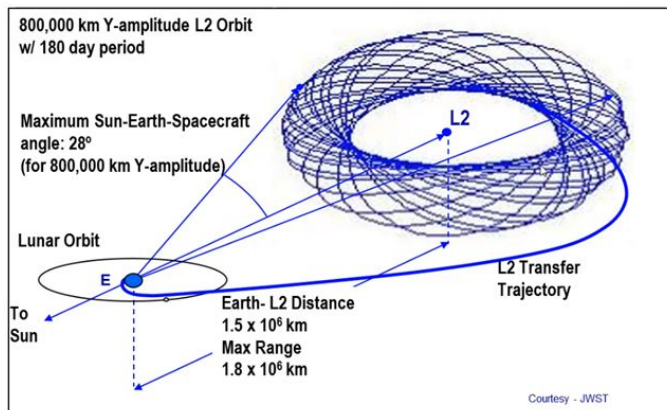


Figure 5.1. The TAP observatory early operations build upon the JWST mission design.

Deployments are completed during the one hundred days of transfer to L2. Antenna boom is released, Sun-shade panels are released and locked, instrument aperture doors are opened, temperature control is enabled, and science calibration is performed. The observatory arrives at L2 ready to proceed to science operations.

5.2 Observatory Design

The observatory design is compatible with a Class B mission, with redundancy and fault tolerance typical of a probe-class mission. The observatory configuration is shown in **Fig 5.2**. The XRT is mounted to an aluminum honeycomb/composite optical bench and, like the Chandra, placed within the central thrust tube with the aperture contained within the 1.6m launch vehicle adapter ring. The IRT and all four WFI detectors are mounted to this common optical bench, allowing convenient alignment during observatory construction. GTM detectors are mounted to afford full and uniform coverage of the sky. During slews and observations, the Sun is maintained in the spacecraft XZ plane. A deployable sun shade shields the optical bench and instruments for sun angles greater than 45 degrees from the spacecraft +X axis. A deployable dual-axis High Gain Antenna (HGA) and two, 3-panel, solar array wings complete the observatory layout.

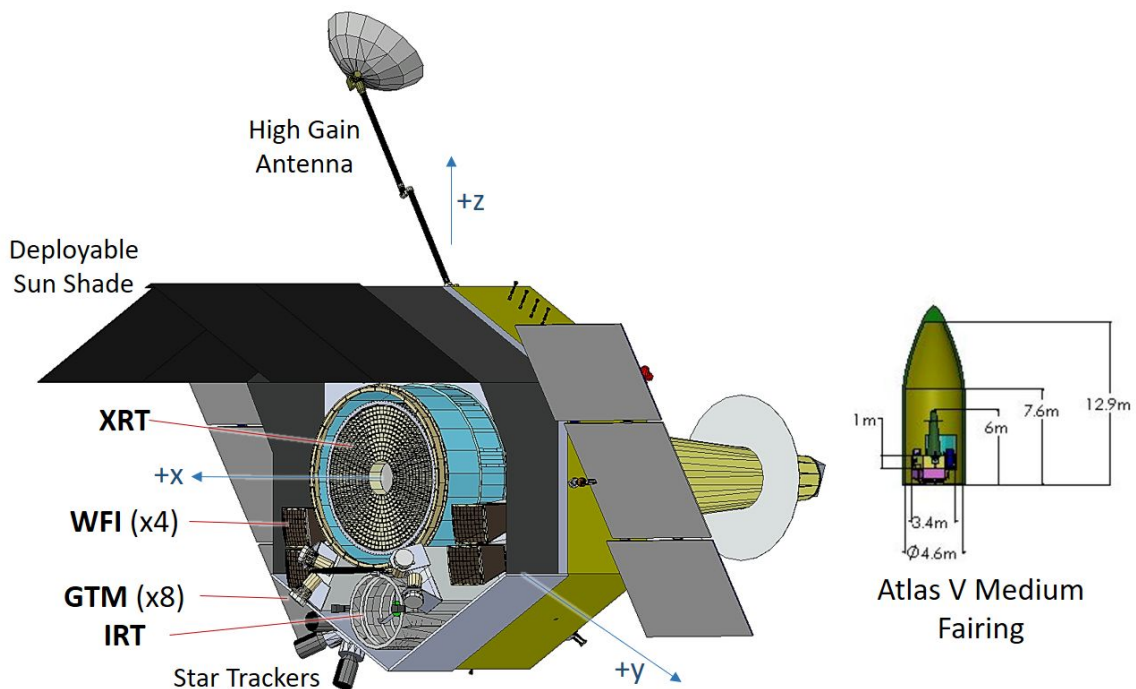


Figure 5.2. The TAP observatory configuration accommodates the instruments on a common optical bench. Two deployable sun shade panels protect them from solar illumination.

5.3 Spacecraft

The spacecraft subsystem architecture is typical for astronomy missions and candidate components are currently available and require no technology development prior to mission PDR.

Mechanical: The mechanical subsystem primarily consists of the hexagonal spacecraft structure, which is 3m from face to face and is 1m tall. A composite thrust tube provides strength to the structure, which is aluminum honeycomb. Mechanisms include the high gain antenna gimbal, boom and hold-down; solar array drives and hold-downs; and deployable sun shade hinges and hold-downs.

Electrical: The TAP electrical subsystem is powered by of a set of two three-panel Triple Junction Gallium Arsenide (Tj GaAs) solar panel wings. An End-of-Life (EOL) power of 1950W is available from the active area of 7.8 m² and predicted efficiency exceeding 29.5% (at 70C). The array is not eclipsed during science operations. A 20 A-hr battery provides power prior to deployment and during peak operations, as required. The Power System Electronics (PSE) provides battery maintenance and high power switching.

Avionics: The avionics subsystem provides control and monitoring of all spacecraft components and science instruments, including autonomous operations necessary for TAP's transient science mission. Using Class B parts and fully redundant electronics, the spacecraft avionics perform data acquisition, processing (including compression), data storage, and transmission to the communications subsystem. Precision on-board timing is provided by available components easily meeting the 100 μsec accuracy needed for TAP science. Processing is performed by a BAE RAD750 processor or equivalent, which is integrated into each of two Integrated Avionics Units (IAU), with one acting as a spare. The IAU also provides low power switching, analog to digital readout of temperature and the Coarse Sun Sensors (CSS) units, timing and clock distribution, and communications with components and the science instruments. Gimbal Control Electronics (GCE) are used to control both the HGA gimbal and the solar array drive. A command Decryption Unit (DU) maintains the security of the command link. The GCE and DU units are internally redundant.

Pointing: The attitude control subsystem (ACS) is comprised of the sensors, control flight software (FSW), and actuators required to point the instrument suite at inertial targets while maintaining solar incidence in the spacecraft XZ plane. A commercially available celestial navigation system uses four star camera heads and inertial rate units to determine orientation of TAP in inertial space. Twenty small CSS are used to detect fault conditions and recover from potential attitude control anomalies. The sensors feed established control algorithms, hosted by the spacecraft avionics, which command the actuators. During science modes, TAP is controlled by six commercially-available (HR-18 or equivalent) reaction wheels, based upon the design of GOES-R. Reaction wheel momentum unloads are expected to occur twice a week (<5 minutes each) and are scheduled with margin to allow them to be interrupted, if necessary, by science targets of opportunity. Short (~5 minute) station-keeping maneuvers once every 1-2 months.

Propulsion: The propulsion subsystem is used to control tip-off rates, to perform the mid-course corrections, and to unload momentum accumulated by the reaction wheels. Two, commercially-available 28" internal diameter diaphragm tanks hold 250 kg of monopropellant at 300 psi (BOL). 24 22N-class rocket engine assemblies provide fully redundant thrust. This traditional blowdown system provides 200 m/s of delta velocity, meeting the needs of TAP with robust margins.

Communications: The dual S- and Ka-band communications subsystem provides a nearly constant command and telemetry link to quickly provide the observatory with ground-initiated targets and to downlink the location of transients that TAP has localized. Commands and low rate telemetry pass through dual omnidirectional S-band antennas connected to an off-the-shelf transponder operating at 5W RF output. Higher rate S-band telemetry can be transmitted by the transponder at 20W RF output through the dual S- and Ka-band 1m HGA. Science data downlinks do not interrupt science operations (because the antennae is gimballed) and are performed roughly once a day using the Ka-band modulator and 10W Solid State Power Amplifier (SSPA) transmitting through the HGA.

Thermal Control: The thermal control subsystem provides cooling for the IRT (90K), WFI (-50C), and XRT (-20C) focal planes, providing passive radiators facing the observatory sun shielded side. The IRT FPA radiator, the largest, is sized to 3.5 m² for a 6W heat load from the IRT (electronics and parasitic heat). Thermal control of the GTM detectors, a low dissipating and room temperature instrument, is provided at each mounting location. Ample area is available from the bus panels to radiate component heat to space at a maximum design temperature of 45C.

5.4 Ground Stations

To support its science objectives, TAP needs to be in nearly continuous contact with a ground station to report on transients discovered with TAP and to report the locations and characteristics of counterparts of transients discovered with TAP or other observatories. Nearly continuous contact is also required so that requests for observations of new TOOs can be uploaded to the spacecraft. In addition, the full telemetry from the observatory needs to be sent to the ground within approximately 24 hours of its generation.

Real-Time Links: The low-latency high-percentage-contact requirement (uplink/downlink for the ToO and transient detections) can be met with a series of 4 S-band 6-m antennas semi-uniformly spread across longitude. The bit rate is in the 1-2 kbps range yielding a downlink time of 10 s for the ~100-byte position-containing packets and ~100 s for the lightcurve, image, and spectrum packets. These 4 ground stations can be drawn from the NASA Near-Earth Network (NEN) and/or from commercial stations. We would negotiate that a 6-m dish and transceiver paid for by the TAP program be installed at these 4 locations. The dish at each station would be dedicated for TAP use during the nominal 6-8 hour window that that station is visible to TAP at L2. During the remainder of the hours each day, the antenna could be used for other contacts at the station's discretion. There are ~5 NASA NEN stations and ~3 commercial or foreign stations that can be utilized. There is a seasonal effect due to latitude that causes dropouts (never longer than 3.25 hrs/day, nearly all days are 0 hrs) which range from 0.5 to 1.1% of the observing time (worst case averaged over 10 years) and can be made to drop to essentially 0.0% if the launch window is constrained.

Full Data Downlink: Ka-band science telemetry is downlinked once per day through schedule contacts with an existing NEN or DSN station. For example, 5.29 Mbps is available through the 18-m NEN station located at White Sands and up to 40 Mbps is available through a 34-m beam waveguide antenna located at a DSN site. Downlinking the expected daily science data volume of 6.2 GB to a DSN site can be

accomplished in as little as 30 minutes per day. On-board storage of 16 GB is available to buffer the science data between contacts.

Ranging: Periodic S-band ranging is accomplished using a larger, existing, Near Earth Network (NEN) antenna and the spacecraft HGA. One of the dedicated 6-m antenna sites could also be increased to 11-m to accomplish this task.

5.5. Operations Centers

The TAP Mission Operations Center (MOC) and Science Operations Center (SOC) control the TAP observatory and execute the science mission. As for other NASA high-energy missions, the High Energy Astrophysics Science Archive Research Center (HEASARC) will archive the final data set.

The MOC performs mission scheduling (including TOO requests), coordinates data flow and contacts with the ground stations, prepares command loads, monitors housekeeping telemetry, and performs health and safety trending and analysis. The MOC also handles the instrument data, preparing the Level 0 data products.

The SOC monitors and trends detailed instrument performance data, validates the science data, processes calibration data, and prepares the Level 1-3 science data products. The SOC also collects and prioritizes TOO requests from contributing observers, include GW alerts, and issues TOO requests to the MOC. Archival data products are rapidly delivered to the HEASARC and made available to the community at large.

6. Concept of Operations

The operations concept for TAP enables its exciting science goals described in §2. The primary requirement for operations is to be able to rapidly respond to scientific opportunities presented by other astronomical observatories or by TAP itself.

Fig. 1.3 shows the expected distribution of observing time by science topic. About 5% of the total time is needed for slewing between targets (§3.4). About 30% of the time is allocated to the follow-up of Ground-based GW Network triggers, and another 10% will be used to observe binary SMBHs detected with LISA. About 15% of the total time will be used to meet the uniformity goals of the all-sky survey with the WFI. Finally, we estimate 5% of the time will be used observing long GRBs, and 35% of the time observing other Time-Domain Astronomy targets (this includes the science goals described in §2.2 as well as TOOs suggested by the broad astronomical community during the TAP mission.)

The rapid TOO response time of the operations centers, continuous communication contact via the ground stations, high sky accessibility of the TAP orbit, the agility of the TAP observatory, and an established network to distribute alerts to an existing follow-up community, combine to make the TAP mission a

powerful window into the transient, high-energy Universe. TAP localizes transients with the WFI and then brings the powerful XRT and IRT instruments to bear for follow-up science.

The halo orbit around L2 provides for high observing efficiency and most of the sky is always immediately available for observations. As described in §5.4, TAP will be nearly continuously in contact with the TAP Mission Operations Center (MOC). This means that commands to observe a new Target of Opportunity (TOO) can be rapidly sent to the spacecraft, and the initial results of such observations can be rapidly sent to the MOC for analysis and distributed to the astronomical community if appropriate. The same link is used to send messages to the ground announcing and characterizing new transients discovered with TAP. The full set of data is sent to the ground approximately daily.

The ground data processing system rapidly processes the initial messages produced by the observatory as well as the full data set. The initial messages provide information about transients discovered on-board as well as results from searches for GW counterparts or other TOO observations. The messages include positions and count rates of interesting sources, thumbnail images of regions of sky near the interesting sources, and light curves. The messages are rapidly and automatically processed in the MOC screened for quality, and distributed through the GCN if appropriate. The processing will evaluate newly discovered transients and make an initial characterization of the new source including the type of transient (sGRB, TDE, nova, etc.). This characterization is sent to on-call staff, who are responsible for drafting a follow-up plan.

Pre-planned WFI X-ray All-sky Survey: The WFI will survey most of the X-ray sky using the observations planned for the IRT and XRT. In addition, TAP will spend 15% of the time on “fill-in” survey targets to increase the uniformity of the sky coverage. A regular grid covering the entire sky with 42 target directions will be used. Typically, 35 of these directions will be available (outside the solar constraint). The “fill-in” time could be used to observe each of the 35 positions for ~300 s daily. Instead, the planning system will concentrate the fill-in time on parts of the sky that have little coverage with non-fill-in observations. Experience with the *Swift* mission, which also emphasized TOOs and rapid response, indicates that there will typically be at least 30 distinct target directions each day (with an average of ~35). With 30 targets, the average TAP observing time would be ~2.0 ks. Deviation from the pre-planned observing schedule will reduce the uniformity of the survey, but this will affect a small fraction of the observing time. The time not pre-planned consists of most of the long GRB observations (5% of the total), a small fraction of the LIGO-Virgo-KAGRA follow-up observations (25%), and (based on *Swift* experience) a small fraction of the TOO time (30%). TAP will easily survey 50% of the sky with an exposure of 700 s daily and 90% of the sky with an exposure of 2000 s weekly. On-board processing of the WFI images determines the brightness and position of X-ray sources within the image and compares that data to the on-board catalog. A new source or a brightness change beyond threshold initiates an on-board TOO request for follow-up with the narrow-field XRT and IRT and, again, immediately downlinks the transient alert data for distribution via the GCN.

XRT and WFI Medium Surveys: The 42 target directions for the “fill-in” WFI survey will produce long exposures for the IRT and XRT. In a year, each of the 42 targets will have an average exposure of ~110 ks distributed in an unpredictable way. In addition, the daily monitoring of a selected LSST Deep

Drilling field (§ 2.2.5) will produce a yearly exposure of ~30 ks for circle on the sky with a diameter of ~3.5 deg.

Monitor the Gamma-ray Sky: The GTM detectors (§4.4) continuously monitor the full sky for transients in the gamma-ray band. When a detection is made, the data from the 8 detectors allows for a coarse localization of the transient, which is typically a GRB. The detection produces on-board TOO request for follow-up using the WFI, XRT, and IRT, and is immediately downlinked as a transient alert via the low-latency S-band telemetry link (§5.4) and sent to the GCN.

Ready for Transient Alerts: (A) As a subscriber to GCN, the TAP SOC (§5.5) receives alerts from GW detectors, neutrino detectors, and transient observers in the EM from all across the globe and in space. The SOC grades these many alerts per day on confidence, filters low confidence alerts for coincidence with others (including alerts from TAP itself), prioritizes the request, builds the search plan, and issues the TOO commands to the MOC (§5.5) for uplink to the observatory. This is a rapid and automated process, requiring only tens of seconds to complete. (B) The world-wide astronomical community will also submit TOO requests for TAP observations through a web site. These will be evaluated by a staff scientist, and implemented if approved by the TAP PI.

Automated Pipeline and Archiving: The complete data stream is processed by the TAP data processing pipeline, converted into FITS files, and posted on the TAP Quick Look website. Searches are made for additional transients and an initial characterization produced. After all the data from an observation have been processed (typically in a week), the data are delivered to the HEASARC for archiving and community access.

Robust Planning System: There will be a new observing plan uploaded to the spacecraft approximately daily (2-day plans on weekends). The plan includes the list of targets, science priority (figure of merit), and instrument configurations. The targets are selected from follow-ups of recent TOOs, monitoring campaigns, and surveys. The plan will be modified as new opportunities, such as GW events, are discovered. It is anticipated that many of the observations in the daily science plan will be bumped by new TOOs. The planning system is aware of the changes, and when possible and appropriate the bumped targets will be rescheduled. The plan for WFI fill-in targets will also be modified.

High Priority TOOs: For some high-priority TOOs, such as GW events, TAP has an automatic response system. For example, when an event candidate is identified by the Ground-based GW Network, the TAP response system will accept inputs describing the likelihood that it is a real GW event, whether it contains a neutron star, and the size and location of the error region. The system then checks constraints, compares priority with current observations, develops an observing strategy, and uploads the revised plan to the spacecraft.

Lower Priority TOOs: The world-wide astronomical community can also submit TOO requests for observation through a web site. These will be evaluated by a staff scientist, and implemented if approved by the TAP PI.

7. Technology

The XRT's mirror assembly is based on the silicon meta-shell X-ray optics technology. It is built up hierarchically in four steps as shown in **Fig 7.1**. The first step is the fabrication of 5,084 mirror segments, by slicing and precision-polishing mono-crystalline silicon and by coating each with 20 nm of iridium to enhance X-ray reflectance. In the second step, the mirror segments are aligned and bonded into 133 mirror modules. Each module, consisting of dozens of mirror segments and a silicon plate serving as its structural backbone, is built up and tested for both meeting science performance requirements, such as effective area and angular resolution at several different energies, and for meeting spaceflight environmental requirements, such as vibrations, acoustics, as well as thermal vacuum. In the third step, the 133 modules are integrated into 5 meta-shells, each consisting of a number of identical modules, ranging from 15 for the innermost meta-shell to 28 for the outermost one. Finally in the last step, the 5 meta-shells are integrated onto a spider using flexures to form the mirror assembly. The flexures linking the meta-shells and the spider serve to isolate the meta-shells both thermally and mechanically from the rest of the observatory.

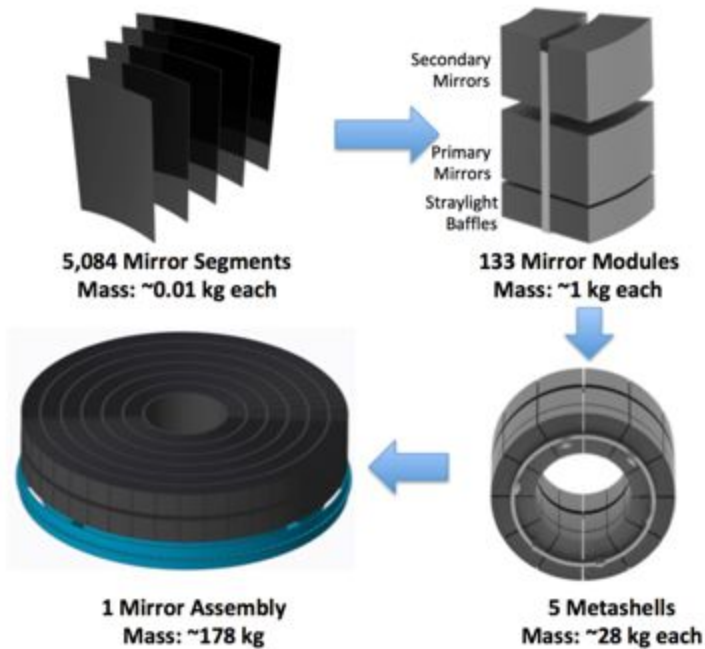


Figure 7.1: *The four major steps of building the XRT mirror assembly. **Upper-left:** fabrication of 5,084 mirror segments. **Upper-right:** Integration of the 5,084 mirror segments to into 133 mirror modules. **Lower-right:** Integration of the 133 mirror modules into 5 meta-shells. **Lower-left:** Integration of the 5 meta-shells into the mirror assembly. The first two steps require new technology, whereas the last two steps require only standard engineering that has been done many times for past missions.*

Of the four steps shown in **Fig 7.1** for building the mirror assembly, the last two are standard engineering processes, requiring no new technology. The first two steps are new and require technology development. As of January 2019, mirror segments (TRL 5) meeting all TAP/XRT requirements, including technical performance as well as schedule and cost, have been made repeatedly. The basic technical elements of the second step, i.e., integration of mirror segments into mirror modules, have also been demonstrated by repeatedly aligning and bonding a pair of primary and secondary mirror segments and subject them to

full-illumination X-ray tests, achieving 2.2" HPD X-ray images, two times better than TAP/XRT requirements.

TRL Raising: We are in the process in procuring necessary tooling to build and test a mirror module with 12 pairs of mirror segments. This mirror module will be subject a set of X-ray performance tests before and after a battery of environmental tests, including vibrations, acoustics, and thermal vacuum. Fully funded by NASA as part of its ROSES Strategic Astrophysics Technology program, we expect to complete this process by December 2020, achieving TRL-6.

8. Risk

We have identified three risks for the TAP mission.

Overlap with other missions/instruments: A challenge for multi-messenger science is that it requires simultaneous (or nearly simultaneous) observations by multiple instruments (flight- and ground-based). There are many existing instruments, planned/approved instruments and missions, and as yet unproposed instruments and missions. It is difficult to know what the operating schedule is with enough certainty to make full use of the synergy with the TAP mission and instruments (which could launch as early as Nov. 2029 (see § 9) or as late as the early 2030s). Currently, LIGO/Virgo will have undergone upgrades (A+ and AdV+) around the middle of the next decade (2024-2025) and then provide continued operations for 4 or 5 years, with KAGRA observations starting in 2021-2022, and LIGO-India added in 2025-2026 (KAGRA and LIGO-India yield significantly smaller error regions of the sky and thus higher detection rates). Given that further LIGO observatory upgrades and third-generation ground-based GW detector designs are under study, we can expect that similar (and/or better) GW instruments will be operating for at least two more decades, allowing high overlap with TAP and enabling its primary science. For LISA the issue of overlap is more difficult to determine, but appears optimistic with a mission launch date under consideration for 2030 to 2034, offering a likely overlap with TAP. PTAs are ongoing experiments whose sources are long-lived (wide orbits will remain so for up to thousands of years), therefore as previously noted concurrent operation with TAP is not a requirement for coordinated science; periodic sources discovered in TAP may be sought with both past, ongoing and future PTAs. The sensitivity of PTAs will improve steadily in the coming decade and beyond, and will improve rapidly with the full coordination of PTAs in Europe (many telescopes), Australia (Parkes), North America (GBT, Arecibo, VLA), India (GMRT), and China (FAST). Timing efforts at these individual telescopes are currently forming into an effective International Pulsar Timing Array. Further rapid sensitivity improvements will come in the era directly preceding the intended TAP launch, as the SKA begins science operations. The SKA starts with 10% of the full array in ~2023, and will grow to the full array in 2030. Over the coming decade, the including of the SKA in the ongoing IPTA program may advance our sensitivity (and detection horizon) on the order of tenfold.

The loss of overlapping missions and projects will of course reduce the amount of observing time spent on those classes of targets, but that time can be reassigned to (a) make longer and/or higher cadence follow-up observations on ToOs transients submitted by other flight missions and ground-based instruments, (b) make follow-up observations on ToOs that would otherwise would not have been

possible, and (c) make higher cadence observations on monitoring targets in the Survey portion of this mission. TAP is designed to be flexible and dynamic -- it can adapt to a wide range of operational domains. With all the pluses and minuses, we believe this to be a low-level risk.

Cost: We have designed a broad-reaching, flexible mission with a set of high-heritage instruments that has a wide range of scientific capabilities, and it fits within the cost-cap of \$1B with a 30% reserve. Should there be cost overruns, we have included a set of descope options (in § 4.5) which can provide up to \$80M in cost reductions with acceptable impact on the science return. We believe this to be a low risk item.

XRT TRL: If there are complications in the design and performance of the XRT Test Mirror and the one Meta-shell (1 of the 5 rings that constitute a full Mirror Assembly) that is run through an entire set of environmental testing (in § 7), then further engineering development may be needed. But given that the current schedule is to have this full-up environment test done by Dec 2020, there is plenty of time to work any remaining development before the start of TAP Phase A (Fig. 9.1). This is a low probability risk.

9. Project Schedule

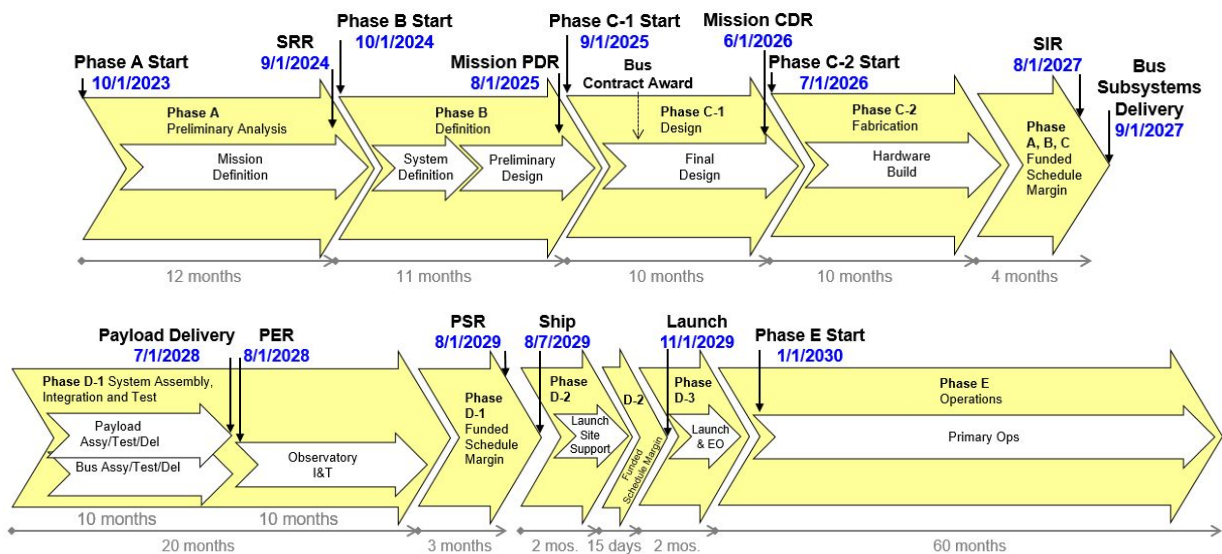


Figure 9.1. The TAP observatory schedule supports a November, 2029 launch, given a start date in October, 2023.

The top-level TAP schedule was developed by the Mission Design Lab at GSFC and shows a credible path meeting the launch readiness date (Fig 9.1). Durations and schedule reserve allocation is consistent with successful previous missions and GSFC design practice. Long-lead components for the TAP instruments, including the CCID-86 (WFI), H4RG/HiViSi (IRT), E2V 231-84 (XRT) detectors, are evolutions of existing designs. Mature interfaces and requirements allow procurement to begin with minimal risk. Technology development for the XRT mirror (§7.0) is already fully funded and underway,

with TRL 6 achieved well before TAP program start. TAP's spacecraft bus components are readily available in industry, lending confidence to the 2-year duration allocated for subsystem delivery. The observatory integration schedule assumes a GSFC in-house spacecraft bus, with integration and test performed at GSFC using existing facilities, including the clean rooms, vibration and thermal vacuum test chambers, and X-ray test laboratories.

Per GPR 7120.7, Schedule Margins and Budget Reserves to be Used In Planning Flight Projects and In Tracking Their Requirements, the schedule includes funded reserve of 1 month/year from confirmation to the start of I&T, 2 months/year during I&T, and 1 week/month during launch site operations, for a total of 227 days.

10. Cost Estimate with Justification

Table 10.1 shows the full TAP mission costs for the nominal and descoped designs. The costs were estimated with the use of a Goddard parametric cost model (PRICE-H) which took as input the TAP Master Equipment List (MEL) generated by the GSFC Mission Design Lab. The MEL includes all the flight hardware needed to realize the TAP mission requirements described in **§3.1 (Science Traceability Matrix)**. The MEL and associated parts costs are shown in the Engineering Concept Definition Package.

In **Table 10.1**, Mgmt refers to Project Management, SE to Systems Engineering, MA to Safety and Mission Assurance, MOS to Mission Operations, and GDS to Ground and Data Systems.

The credibility of the cost estimate comes from two factors. First, the TAP mission requires minimal technology development (**§7**); thus most costs may be estimated directly and unambiguously from the hardware design. Second, there exists considerable independently reviewed proposal heritage for the TAP instruments, including ISS-TAO (WFI), Star-X (XRT), Exist (IRT), as well as actual cost heritage including numerous industrial IRT designs, *Swift* (spacecraft), and Fermi-GBM (GTM).

As shown in the final row of **Table 10.1**, the TAP mission cost of \$1028M is consistent with the Probe cost cap (\$1B), to within the accuracy of the Mission costing process, roughly estimated at 20%. This cost was independently verified by the Goddard Resource Analysis Office (RAO) at the 15% level. Table 10.1 also shows the cost of the descoped mission (**§4.5**), which includes the following changes from the baseline mission: reduction of the number of WFI modules from 4 to 3; reduction of the IRT diameter from 70 to 60 cm; and reduction of the XRT effective area by 30%. **Table 10.1** shows that the descoped mission saves \$76M while still providing a compelling science program (see **Table 4.2**).

Table 10.1: Master Equipment List Based Parametric Total Lifecycle Cost Estimate for Baseline and Descope mission configurations.

PROJECT PHASE	TAP WBS/Sub-system	TAP Mission (Baseline) COST [FY18 \$M]	TAP Mission (Descoped) COST [FY18 \$M]
Phase A		\$35	\$33
Phases B-D	Mgmt, SE, MA	\$86	\$79
	Science	\$25	\$23
	X-ray Telescope (XRT)	\$70	\$57
	Wide-Field Imager (WFI)	\$91	\$75
	Infrared Telescope (IRT)	\$103	\$93
	Gamma-ray Transient Monitor (GTM)	\$24	\$24
	Spacecraft, including ATLO	\$125	\$125
	MOS/GDS	\$31	\$28
	Launch Vehicle and Services	\$150	\$150
	Reserves	\$212	\$196
	Total Cost Phases B-D	\$917	\$850
Phase E-F	Operations	\$66	\$60
	Reserves	\$10	\$9
	Total Cost Phases E-F	\$76	\$69
	TOTAL LIFECYCLE COST	\$1,028	\$952
- This parametric cost estimate is based on the Probe's Master Equipment List derived from the Final Engineering Concept Definition Package that accurately reflects the mission described in the Probe's Final Report. This estimate is to be used only for non-binding rough order of magnitude planning purposes.			
- Team X estimates are generally model-based, and were generated after a series of instrument and mission level studies. Their accuracy is commensurate with the level of understanding typical to Pre-Phase-A concept development. They do not constitute an implementation or cost commitment on the part of JPL or Caltech.			

List of Participants

Jordan Camp (GSFC), Josh Abel (GSFC), Scott Barthelmy (GSFC), Mark Bautz (MIT), Ehud Behar (Technion, Israel), Edo Berger (Harvard U), Sarah Burke-Spolaor (West Virginia U), S. Bradley Cenko (GSFC), Neil Cornish (Montana State U), Tito Dal Canton (GSFC), Christopher Fryer (LANL), Suvi Gezari (U Maryland), Paul Gorenstein (SAO), Sylvain Guiriec (GW U), Dieter Hartmann (Clemson U), Vicky Kalogera (Northwestern U), Jeffrey Kruk (GSFC), Alexander Kuttyrev (GSFC), Raffaella Margutti (Northwestern U), Francis Marshall (GSFC), Brian Metzger (Columbia U), Cole Miller (U Maryland), Scott Noble (GSFC), Jeremy Perkins (GSFC), Andrew Ptak (GSFC), Bill Purcell (Ball Aerospace), Judith Racusin (GSFC), Joshua Schlieder (GSFC), Jeremy Schnittman (GSFC), Alberto Sesana (U Birmingham), Peter Shawhan (U Maryland), Leo Singer (GSFC), Alexander van der Horst (GWU), Richard Willingale (U Leicester), Kent Wood (NRL), William Zhang (GSFC).

References

- Aartsen, M. G. et al. (2013) “First Observation of PeV-Energy Neutrinos with IceCube” *PRL*, 111, 021103
- Aartsen, M. G. et al. (2018) “Multimessenger observations of a flaring blazar coincident with high-energy neutrino IceCube-170922A”, *Science* 361, eaat1378.
- Abbott et al. (2017a) “GW170817: Observation of Gravitational Waves from a Binary Neutron Star Inspiral”, *PRL*, 119, 1101
- Abbott et al. (2017b) “Multi-messenger Observations of a Binary Neutron Star Merger”, *ApJL* 848, 12
- Abbott et al. (2017c), “Gravitational Waves and Gamma-Rays from a Binary Neutron Star Merger: GW170817 and GRB 170817A” *ApJL*, 848, L13
- Abbott, B. P., et al. (2018) “Prospects for observing and localizing gravitational-wave transients with Advanced LIGO, Advanced Virgo and KAGRA”, *Living Rev. in Relativity*, 21, 3
- Alexander, K. D., et al, (2018) “A Decline in the X-ray through Radio Emission from GW170817 Continues to Support an Off-axis Structured Jet”
- Angel, J. (1979) “Lobster Eyes as X-ray Telescopes” *ApJ* 233 364
- Bauswein, A. et al. (2012) “Equation-of-state dependence of the gravitational-wave signal from the ring-down phase of neutron-star mergers” *PRD*, 86, 063001
- Beckmann, V. & Schrader, C. R. (2012) “Active Galactic Nuclei” ISBN-13: 978-3527410781. Wiley-VCH Verlag GmbH
- Berger, E., Fong, W., & Chornock, R. (2013) “An r-process Kilonova Associated with the Short- hard GRB 130603B” *ApJL*, 774, L23
- Bloom, J. S., et al. (2011) “A Possible Relativistic Jetted Outburst from a Massive Black Hole Fed by a Tidally Disrupted Star” *Science*, 333, 203
- Bowen, D. B. et al. (2018) “Quasi-periodic Behavior of Mini-disks in Binary Black Holes Approaching Merger” *ApJL* 853, 17
- Breedt, E. et al. (2010) “Twelve years of X-ray and optical variability in the Seyfert galaxy NGC 4051” *MNRAS*, 403, 605
- Burrows, D. N. et al. (2011) “Relativistic jet activity from the tidal disruption of a star by a massive black hole” *Nature* 476, 421
- Cannon, K., et al, (2012) “Toward Early-warning Detection of Gravitational Waves from Compact Binary Coalescence” *ApJ* 748 136
- Chan, M.l., et al, (2018) “Binary neutron star mergers and third generation detectors: Localizations and early warning”, *PRD* 97, 123014
- Chornock, R. (2014) “GRB 140515A at $z=6.33$: Constraints on the End of Reionization from a Gamma-Ray Burst in a Low Hydrogen Column Density Environment”, *astroph/1405.7400*
- Cooray, A. (2004) “Gravitational-wave background of neutron star-white dwarf binaries”, *MNRAS* 354, 25
- Cornelisse, R. et al. (2003) “Six years of BeppoSAX Wide Field Cameras observations of nine galactic type I X-ray bursters” *A&A*, 405, 1033
- Cucchiara et al. (2011) “A Photometric Redshift of $z \sim 9.4$ for GRB 090429B”, *ApJ* 736, 7
- Dal Canton et al. (2019) “Detectability of modulated X-rays from LISA's supermassive black hole mergers” eprint arXiv:1902.01538

- D'Ascoli et al. (2018)* “Electromagnetic Emission from Supermassive Binary Black Holes Approaching Merger” *ApJ*, **865**, 140
- Eichler, D. et al. (1989)*, “Nucleosynthesis, neutrino bursts and gamma-rays from coalescing neutron stars”, *Nature*, 340, 126
- Ferrarese et al. (2000)* “A Fundamental Relation between Supermassive Black Holes and Their Host Galaxies”, *ApJ*, 539L, 9
- Filippenko (1997)* “Optical Spectra of Supernovae”, *ARA&A*, 35, 309
- Fraser, G. et al. (2010)* “The Mercury imaging X-ray spectrometer (MIXS) on BepiColumbo” *Planetary & Sp.Sci.*, 58, 79
- Fryer et al. (1999)*, “Merging White Dwarf/Black Hole Binaries and Gamma-Ray Bursts”, *ApJ*, 520, 650
- Gebhardt, K. et al. (2000)*, “A Relationship between Nuclear Black Hole Mass and Galaxy Velocity Dispersion”, *ApJ* 539, L13
- Gezari, S. et al. (2008)* “UV/Optical Detections of Candidate Tidal Disruption Events by GALEX and CFHTLS” *ApJ*, 676, 944
- Goldstein, A. et al. (2017)* “An Ordinary Short Gamma-Ray Burst with Extraordinary Implications: Fermi-GBM Detection of GRB 170817A”, *ApJL*, 848, 14
- Haiman, Z. (2017)* “Electromagnetic chirp of a compact binary black hole: A phase template for the gravitational wave inspiral”, [PhRvD..96b3004H](https://arxiv.org/abs/1708.07253)
- Hallinan, G. et al. (2017)* “A radio counterpart to a neutron star merger”, *Science* 358, 1579
- Holoien, T. et al. (2016)* “Six Months of multiwavelength follow-up of the tidal disruption candidate ASASSN-14li and implied TDE rates from ASAS-SN”, *MNRAS* 455, 2918
- Janka, H.-T. et al. (1999)* “Black Hole-Neutron Star Mergers as Central Engines of Gamma-Ray Bursts” *ApJ*, 527, L39
- Kasen, D. (2010)* “Seeing The Collision Of A Supernova With Its Companion Star” *ApJ* 708 1025
- Keek, L. et al. (2010)* “Multi-Instrument X-Ray Observations Of Thermonuclear Bursts With Short Recurrence Times” *ApJ*, 718, 292
- Kelley, L. et al. (2018)* “Massive BH Binaries as Periodically-VARIABLE AGN” eprint arXiv:1809.02138
- Klein, A. et al. (2016)* “Science with the space-based interferometer eLISA: Supermassive black hole binaries” *PRD* **93**, 024003
- Körding, E.G., Migliari, S., Fender, R., et al. (2007)* “The variability plane of accreting compact objects” *MNRAS*, 380, 301
- Korol, V. et al. (2017)* “Prospects for detection of detached double white dwarf binaries with Gaia, LSST, and LISA” *MNRAS* 470, 1894
- Li et al. (2011)* “Nearby supernova rates from the Lick Observatory Supernova Search - III. The rate-size relation, and the rates as a function of galaxy Hubble type and colour”, *MNRAS*, 412, 1473
- Lien, A. et al. (2014)* “Probing The Cosmic Gamma-Ray Burst Rate With Trigger Simulations Of The Swift Burst Alert Telescope” *ApJ* 783, 24
- LSC Instrument Whitepaper*, <https://dcc.ligo.org/LIGO-T1800133/public>
- LSC et al (2017)* *Multimessenger Observations of a Binary Neutron Star Merger*, *ApJ Letters* 828:L12
- Markowitz, A., & Edelson, R. (2004)* “An Expanded Rossi X-Ray Timing Explorer Survey of X-Ray Variability in Seyfert I Galaxies” *ApJ*, 617, 939
- McClelland, R.S. et al. (2017)* “The STAR-X X-ray Telescope Assembly (XTA)” *SPIE Proc.* 10399, 1039908

- McHardy, I. M., Koerding, E., Knigge, C., Uttley, P., & Fender, R. P. (2006) “Active galactic nuclei as scaled-up Galactic black holes” *Nature*, 444, 730
- McQuinn et al., (2008) *MNRAS*, 388
- Meszáros, P. (2017) “Astrophysical Sources of High-Energy Neutrinos in the IceCube Era” *Annual Rev. of Nuclear and Particle Science*, 67, 45
- McQuinn, M. et al (2008) “Probing the neutral fraction of the IGM with GRBs during the epoch of reionization” *Monthly Notices of Royal Astronomical Society*, 388, 1101
- Metzger, B.D. (2012), “Nuclear-dominated accretion and subluminal supernovae from the merger of a white dwarf with a neutron star or black hole”, *MNRAS* 419, 827
- Metzger, B. (2017) “Kilonovae” *Living Reviews in Relativity*, 20, Issue 1, 3, pp. 59
- Mingarelli et al. (2017) “The local nanohertz gravitational-wave landscape from supermassive black hole binaries”, *Nature Astronomy* 1, 886
- Narayan, R. et al. (1992) “Gamma-ray bursts as the death throes of massive binary stars”, *ApJ* 395, 83
- Nynka, M. et al, (2018) “Fading of the X-Ray Afterglow of Neutron Star merger GW170817/GRB 170817A at 260 Days”, *ApJ* 862, L19
- Osten, R. et al. (2007) “Nonthermal Hard X-ray Emission and Iron K- α Emission from a Superflare on II Pegasi”, *ApJ* 654, 1052
- Osten, R. et al. (2010) “The Mouse That Roared: A Superflare from the dMe Flare Star EV Lac Detected by Swift and Konus-Wind”, *ApJ* 721, 785
- Paczynski, B. (1991) “Cosmological gamma-ray bursts”, *Acta Astro.* 41, 257
- Padovani et al. (2007) “The Deep X-ray Radio Blazar Survey. III. Radio Number Counts, Evolutionary Properties, and Luminosity Function of Blazars”, *ApJ* 662, 182
- Peretz & Behar (2018) “Classifying AGN by X-ray hardness variability”, *MNRAS* 481, 3563
- Perlmutter et al. (1999) “Measurements of Ω and Λ from 42 High-Redshift Supernovae”, *ApJ* 517, 565
- Piro, A. L., Chang, P., & Weinberg, N. N. (2010) “Shock Breakout from Type Ia Supernova” *ApJ*, 708, 598
- Rees, M. (1988) “Tidal disruption of stars by black holes of 10^6 to 10^8 solar masses in nearby galaxies”, *Nature* 333, 523
- Riess et al. (1998) “Observational Evidence from Supernovae for an Accelerating Universe and a Cosmological Constant”, *AJ* 116, 1009
- Ruffert, M. & Janka, H., “Gamma-ray bursts from accreting black holes in neutron star mergers” *A&A* 1999, 344, 573
- Salvaterra, R. et al. (2009) “GRB 090423 at a redshift of $z \sim 8.1$ ” *Nature*, 461, 1258
- Sari, R. (1998) “The Observed Size and Shape of Gamma-Ray Burst Afterglow”, *ApJ* 494, L49
- Schnittman, J. D. (2014) “Coordinated Observations with Pulsar Timing Arrays and ISS-Lobster” *arXiv:1411.3994*
- Shafter, A. W. (1997) “On the Nova Rate in the Galaxy”, *ApJ*, 487, 226
- Soderberg, A. (2008) “An extremely luminous X-ray outburst at the birth of a supernova”, *Nature* 453, 469
- Tanaka et al. (2012) “Detectability of high-redshift superluminous supernovae with upcoming optical and near-infrared surveys”, *MNRAS*, 422, 2675
- Tanvir, N. et al. (2009) “A gamma-ray burst at a redshift of $z \sim 8.2$ ” *Nature*, 461, 1254

- Tanvir, N. R., et al. (2013) “A ‘kilonova’ associated with the short-duration γ -ray burst GRB 130603B” *Nature*, 500, 547
- Taylor, S. R., et al. (2016) “Are we there yet? Time to detection of nanohertz gravitational waves based on pulsar-timing array limits” *ApJL*, 819, 6
- Thompson, T. et al. (2009) “A New Class of Luminous Transients and a First Census of their Massive Stellar Progenitors”, *AJ* 705, 1364
- Troja, N., et al., (2017) “The X-ray counterpart to the gravitational-wave event GW170817”, *Nature* 551, 71
- Troja, N., et al., (2018) “The outflow structure of GW170817 from late-time broad-band observations”, *MNRAS* 478, L18
- Tsang, D., Read, J. S., Hinderer, T., Piro, A. L., & Bondarescu, R. (2012) “Resonant Shattering of Neutron Star Crusts” *Physical Review Letters*, 108, 011102
- van Velzen, S., et al. (2016) “Discovery of Transient Infrared Emission from Dust Heated by Stellar Tidal Disruption Flares”, *ApJ* 829, 19
- van Velzen, S. et al. (2018) “On the Mass and Luminosity Functions of Tidal Disruption Flares: Rate Suppression due to Black Hole Event Horizons”, *ApJ*, 852, 72
- Vigeland et al., submitted
- Waxman, E. & Katz, B. (2017) “Shock Breakout Theory”, in *Handbook of Supernovae*, Springer
- Zauderer et al. (2011) “Birth of a relativistic outflow in the unusual gamma-ray transient Swift J164449.3+573451”, *Nature* 476, 425.
- Zhang, W. et al. (2018) “Astronomical X-ray Optics Using Mono-crystalline Silicon: High Resolution, Light Weight, and Low Cost”, *SPIE Proc.* 10699, 1069900
- URL#1: <https://dcc.ligo.org/public/0125/T1600119/004/wp2016.pdf>
- URL#2: **arXiv:astro-ph/0310889v1** OR <https://inspirehep.net/record/632072>
- URL#3: <https://dcc.ligo.org/LIGO-T1800133/public>

Acronyms

ACS	Attitude Control Subsystem	FSM	Fast Steering Mirror
AGILE	Astro-Rivelatore Gamma a Immagini Leggero	FWHM	Full Width at Half Maximum
AGN	Active Galactic Nuclei	GALEX	Galaxy Evolution Explorer
ANTARES	Astronomy with a Neutrino Telescope And Abyss environmental REsearch	GBM	Gamma-ray Burst Monitor (on <i>Fermi</i>)
ATHENA	Advanced Telescope for High Energy Astrophysics	GBT	Green Bank Telescope
ATLO	Assembly, Test, and Launch	GCE	Gimbal Control Electronics
BATSE	Operations	GCN	Gamma-ray Coordinates Network
BH	Burst & Transient Source Experiment	GEVS	General Environmental Verification Standard
BNS	Black Hole	GmbH	Gesellschaft mit beschränkter Haftung
BOL	Binary Neutron Star	GMRT	Giant Metrewave Radio Telescope
CBE	Beginning of Life	GOES	Geostationary Operational Environmental Satellite Network
CCD	Current Best Estimate	GRB	Gamma-Ray Burst
ccSN	Change Coupled Device	GSFC	Goddard Space Flight Center
CFHTLS	Core-collapse supernova Canada-France-Hawaii Telescope	GTM	Gamma-ray Transient Monitor
CGRO	Legacy Survey	GW	Gravitational Wave
CHIME	Compton Gamma-Ray Observatory Canadian Hydrogen Intensity Mapping Experiment	HEASARC	High Energy Astrophysics Science Archive Research Center
CMB	Experiment	HESE	High-Energy Starting Events
CSS	Cosmic Microwave Background	HiViSi	Hybrid Visible Silicon Imager
DSN	Coarse Sun Sensor	HPD	Half Power Diameter
EELV	Deep Space Network	H4RG	Hawaii 4k, R denotes Reference pixels, and G denotes Guide windows
EM	Evolved Expendable Launch Vehicle	IGM	InterGalactic Medium
EMRI	Electro-Magnetic	IPTA	International Pulsar Timing Array
EOL	Extreme Mass Ratio Inspiral	IRT	Infrared Telescope
EOS	End of Life	ISM	InterStellar Medium
EPTA	Equation of State	JPL	Jet Propulsion Laboratory
eROSITA	European Pulsar Timing Array extended ROentgen Survey with an	JWST	James Webb Space Telescope
FAST	Imaging Telescope Array 500-meter Aperture Spherical radio Telescope	KAGRA	Kamioka Gravitational Wave Detector
FITS	Telescope	L2	Lagrange point 2
FoR	Flexible Image Transport System	LAT	Large Area Telescope (on <i>Fermi</i>)
FoV	Field of Regard	LIGO	Laser Interferometer Gravitational-wave Observatory
FPA	Field of View Focal Plane Assembly		

LISA	Laser Interferometer Space Antenna	SKA	Square Kilometer Array
LOFAR	LOW Frequency ARray	SM	Secondary Mirror
LSST	Large Synoptic Survey Telescope	SMBH	Supermassive Black Hole
MCO	Micro-Channel Optic	SMBHB	Supermassive Black Hole Binary
MDL	Mission Design Laboratory	SNe	Supernovae
MEB	Main Electronics Box	SOC	Science Operations Center
MEL	Master Equipment List	SSPA	Solid State Power Amplifier
MEV	Maximum Expected Value	STM	Science Traceability Matrix
MIXS	Mercury Imaging X-ray Spectrometer	TAO	Transient Astrophysics Observatory
MMA	Multi-Messenger Astronomy	TAP	Transient Astrophysics Probe
MOC	Mission Operations Center	TDE	Tidal Disruption Event
MOSFIRE	Multi-Object Spectrometer for Infra-Red Exploration	TESS	Transiting Exoplanet Survey Satellite
NaI	Sodium Iodide	TOO	Target of Opportunity
NANOGrav	North American Nanohertz Observatory for Gravitational Waves	TRL	Technology Readiness Level
NEN	Near-Earth Network	TTV	Transit-Timing Variations
NS	Neutron Star	UHE	Ultra High Energy
NSBH	Neutron Star Black Hole	UV	Ultraviolet
NSF	National Science Foundation	UVOT	Ultraviolet/Optical Telescope (on <i>Swift</i>)
OBF	Optical Blocking Filter	VLA	Very Large Array
OTA	Optical Telescope Assembly	WFI	Wide-Field Imager
PAF	Payload Adapter Fitting	WFIRST	Wide Field Infrared Survey Telescope
PM	Primary Mirror	WMAP	Wilkinson Microwave Anisotropy Probe
PMT	Photomultiplier Tube	XRT	X-ray Telescope
PPTA	Parkes Pulsar Timing Array		
PSE	Power System Electronics		
PTA	Pulsar Timing Array		
RAO	Resource Analysis Office		
RASS	ROSAT All Sky Survey		
RoC	Radius of Curvature		
ROSAT	ROentgen SATellite		
ROSES	Research Opportunities in Earth and Space Science		
RXTE	Rossi X-ray Timing Explorer		
S/C	Spacecraft		
SCA	Sensor Chip Assembly		
sGRB	short Gamma-Ray Burst		
SiPM	Silicon Photomultiplier		